Passive Full-Wave MOSFET Rectifiers for Electromagnetic Harvesting

by

Mehmet Yilmaz

A thesis
presented to the University of Waterloo
in fulfillment of the
thesis requirement for the degree of
Master of Applied Science
in
Electrical and Computer Engineering

Waterloo, Ontario, Canada, 2013

© Mehmet Yilmaz 2013

I hereby declare that I am the sole author of this thesis. This is a true copy of the thesis, including any required final revisions, as accepted by my examiners.
I understand that my thesis may be made electronically available to the public.

ABSTRACT

A new generation of electronic devices has emerged microwatt-level power supplies to operate. Thanks to micro-power processors and sensors, micro-power sources have become an attractive option for industry and research.

This work focuses on micro-power sources that harvest vibrational energy by deploying electrostatic, electromagnetic, and piezoelectric transduction techniques. The output power of vibrational energy harvesters is in AC form, whereas electronic loads require known DC power supplies to operate. Thus, there is a need for AC-DC conversion between harvesters and electronic loads.

Traditional full-wave bridge rectifiers and center-tapped transformer rectifiers are not feasible in microwatt-level harvesters, as low output power undermines their power efficiency. Thus, rather than traditional rectifiers, novel low-power, high efficiency conversion circuits are required. This goal is particularly challenging when it comes to electromagnetic energy harvesters, since their output voltage is much lower than that of electrostatic and piezoelectric harvesters

In this work, we studied four different full-wave rectifiers; a silicon diode bridge rectifier, a Schottky diode bridge rectifier, a passive MOSFET rectifier, and an active MOSFET rectifier. Through simulation results, we found the voltage and power efficiency of each rectifier. We found that MOSFET-type rectifiers were better than diode type rectifiers in terms of both voltage and power efficiency. Both full-wave MOSFET rectifiers have about 99% voltage and power efficiency. There is only a small difference in power and voltage efficiency between the two MOSFET types below an input voltage amplitude of 600 mV.

Since an active MOSFET rectifier has extra components and the need of an external DC supply to power its active devices, we concluded it was not a good option for small scale harvester systems. We implemented the passive MOSFET rectifier, tested its performance in rectifying the output of an electromagnetic harvester, and analysed its effects on the harvester's performance.

When we connected the rectifier to the harvester, it doubled the optimum load from 24 Ω to 48 Ω. We also studied the rectifier's effect on harvester natural frequency, and found it changed little, which means our rectifier acts like resistance.We also calculated the power efficiency based on harvester tests, and found we achieved a maximum 74% power efficiency.

Acknowledgements

I would like to thank and acknowledge my mentors, and friends, who helped me through my study and work at the University of Waterloo, where I dedicate a special thanks to my supervisors Dr. Mustafa Yavuz, Dr.Baris Fidan, and Dr.Ramadan El-Shatshat for their support and guidance during the program of study.

Also I would like to acknowledge and thank Dr.Eihab Abdel-Rahman, Dr. M.A.E Mahmoud, Dr. M.S.M Soliman, Dr. Sangtak Park, and Karim El-rayes for many things I have learned from them during the program of study.

Last but not least, I would like to thank my family for their priceless love, support and encouragement during my education life.

Dedication

To my lovely ones... You inspired me with every step I have taken.

Contents

List of Figures viii

List of Tables x

1 Introduction 1
1.1 Motivation . . . 1
1.2 Energy Harvesting . . . 1
1.2.1 Energy Harvesting Basics . . . 2
1.3 Scales of Energy Harvesting . . . 3
1.4 Types of Energy Harvesting . . . 4
1.4.1 Solar Energy Harvesting . . . 5
1.4.2 Thermal Energy Harvesting . . . 7
1.4.3 Kinetic Energy Harvesting . . . 8
1.4.3.1 Piezoelectric . . . 9
1.4.3.2 Electrostatic . . . 11
1.4.3.3 Electromagnetic . . . 13
1.5 Thesis Outline . . . 14

2 Power Management in Vibration-Based Energy Harvesters 16
2.1 Power Conditioning . . . 16
2.2 Maximum Power Transfer Theorem in Harvesters . . . 17
2.3 Common Components Used in Rectification . . . 19
2.3.1 Diodes . . . 19
2.3.2 Transformers . . . 21
2.3.3 Capacitors . . . 23
2.4 AC-DC Conversion . . . 24
2.4.1 Passive and Active AC-DC Conversion . . . 24
2.4.2 Half-Wave Rectifier . . . 25
2.4.3 Full-Wave Rectifiers . . . 27
2.4.3.1 Full-Wave Center-Tapped Transformer Rectifier . . . 27
2.4.3.2 Full-Wave Bridge Rectifier . . . 29
2.4.4 The Smoothing Capacitor . . . 30

3 Implementing MOSFET Rectifiers **31**
3.1 Introduction . . . 31
3.2 Types of MOSFETs . . . 32
3.3 Passive Full-Wave MOSFET Rectifiers . . . 35
3.4 Active Full-Wave MOSFET Rectifiers . . . 37
3.5 Baseline Testing of the Passive Full-Wave MOSFET Rectifer . . . 39
3.5.1 Simulations of Different Full-wave Bridge Rectifier Types in LTspice IV . . . 40
3.5.1.1 Full-Wave Silicon Diode Bridge Rectifier . . . 40
3.5.1.2 Full-wave Schottky Diode Bridge Rectifier . . . 41
3.5.1.3 Full-Wave Passive MOSFET Bridge Rectifier . . . 42
3.5.1.4 Full-Wave Active MOSFET Bridge Rectifier . . . 44
3.6 Comparison of Full-wave Rectifiers Simulation Results . . . 47
3.7 Testing A Passive Full-Wave MOSFET Rectifier With Function Generator . . . 50
3.8 Testing of Active Full-Wave MOSFET Rectifier With Function Generator . . . 54

4 Passive MOSFET Rectification in Electromagnetic Harvesters **56**
4.1 Maximum Power Extraction in Electromagnetic Harvester . . . 56
4.1.1 Optimum Load Measurements of the Harvester With and Without Rectifier Circuitry . . . 58
4.1.2 Impedance Measurements for the Passive MOSFET Rectifier 60
4.2 Testing the Passive MOSFET Rectifier With Harvester . . . 63
4.3 Implementation of the Passive MOSFET Rectifier on the Printed Circuit Board(PCB) . . . 63

5 Conclusion and Future Work **68**
5.1 Conclusion . . . 68
5.2 Future Work . . . 69

References **70**

List of Figures

1.1 Different types of harvestable energy sources [4] 2
1.2 General energy harvesting system phases 3
1.3 Typical solar harvester system[4] 5
1.4 Electrical model of a PV module 6
1.5 Illustration of operation mechanism of a TEG [19] 8
1.6 Model of a mass-spring-damper system for vibration based energy harvesters 10
1.7 Piezoelectric cantilever beam structure generator 10
1.8 A typical electrostatic energy harvest [23] 13

2.1 Power flow from environment to electronic load 17
2.2 The circuit with an AC current source 17
2.3 The circuit with an AC voltage source 18
2.4 Representation of a semiconductor diode 19
2.5 $i - v$ characteristic of a diode 20
2.6 Basic transformer structure and windings [23] 22
2.7 Ideal transformer circuit diagram [34] 22
2.8 Parallel plate capacitor structure 23
2.9 Half wave rectifier circuit diagram 25
2.10 Half wave rectifier outputs a) ideal diode condition, b) real diode condition [32] 26
2.11 Full-wave center-tapped transformer rectifier 28
2.12 AC input and rectified output wave forms of full-wave rectifier . . . 28
2.13 Full-wave bridge rectifier 29
2.14 Full-wave bridge rectifier [35] 30

3.1 MOSFET types; a)P-type MOSFET, b) N-type MOSFET 32
3.2 MOSFET characteristic I-V curves [33] 33
3.3 Saturation region characteristic 33
3.4 MOSFET cut-off characteristic 34
3.5 Illustration of MOSFET parasitic capacitances 34
3.6 Full-wave passive MOSFET rectifier circuit 35
3.7 Full-wave passive MOSFET rectifier circuit on the breadboard . . . 37
3.8 Full-wave active MOSFET rectifier circuit 38
3.9 Full-wave active MOSFET rectifier circuit on the breadboard 39
3.10 Full-wave silicon diode bridge rectifier 41

3.11 V_{in} and V_{out} signals of full-wave silicon diode bridge rectifier, V_{in}=1V, R_L=1 kΩ, f=100Hz 41
3.12 Full-wave Schottky diode bridge rectifier 43
3.13 V_{in} and V_{out} signals of full-wave Schottky diode bridge rectifier, V_{in}=1V, R_L=1 kΩ, f=100Hz 43
3.14 Full-wave passive MOSFET bridge rectifier 45
3.15 V_{in} and V_{out} signals of full-wave passive MOSFET rectifier, V_{in}=800 mV, R_L=1 kΩ, f=100Hz 45
3.16 Full-wave active MOSFET bridge rectifier 47
3.17 V_{in} and V_{out} signals of full-wave active MOSFET rectifier, V_{in}=800 mV, R_L=1 kΩ, f=100Hz 47
3.18 Voltage efficiency comparison of rectifiers 49
3.19 Power efficiency comparison of rectifiers 50
3.20 Rectified signal for the 300 mV input amplitude 51
3.21 Rectified signal for the 850 mV input amplitude 51
3.22 Rectified signal for the 500 mV input amplitude 54

4.1 Frequency-response curves for the electromagnetic harvester: a) harvester alone, b) rectifier connected to harvester and R_L=1 kΩ load, c) rectifier connected but no load. 57
4.2 Optimum load test setup with rectifier circuit 58
4.3 Optimum load graph without rectifier circuit 59
4.4 Optimum load graph with rectifier circuit 60
4.5 Input impedance measurement test schematic 61
4.6 Input impedance Z_{in} vs frequency, when the output is an open circuit 61
4.7 Input impedance Z_{in} vs frequency with a resistive load at the output of the rectifier 62
4.8 Power efficiency vs acceleration amplitude (g) for passive MOSFET rectifier 64
4.9 PCB layout of passive MOSFET rectifier 65
4.10 Fabricated PCB of passive MOSFET rectifier and toonie 65
4.11 PCB assembly of passive MOSFET rectifier 66
4.12 Input and output signals of the PCB test 66
4.13 Capacitor added to PCB and toonie 67
4.14 Input and output signals when capacitor added to passive MOSFET rectifier 67

List of Tables

3.1 Full-wave silicon diode bridge rectifier input and output voltage amplitudes, as well as voltage and power efficiency, for R_L=1 kΩ, f=100Hz. 42
3.2 Full-wave Schottky diode bridge rectifier input and output voltage amplitudes, as well as voltage and power efficiency, for R_L=1 kΩ, f=100Hz. 44
3.3 Full-wave passive MOSFET bridge rectifier input and output voltage amplitudes, with voltage and power efficiency, for R_L=1 kΩ, f=100Hz. 46
3.4 Full-wave active MOSFET bridge rectifier input and output voltage amplitudes, with voltage and power efficiency, for R_L=1 kΩ, f=100 Hz. 48
3.5 Full-wave passive MOSFET rectifier input and output voltage values and voltage efficiency, using a function generator 52
3.6 Full-wave passive MOSFET rectifier input voltage values and power efficiency using a function generator 53
3.7 Full-wave active MOSFET rectifier input and output voltage values, as well as voltage and power efficiency, as tested with a function generator 55

4.1 Full-wave passive MOSFET rectifier input/ output voltage amplitudes and voltage efficiency test results as tested with a harvester . 63

Chapter 1

Introduction

1.1 Motivation

Energy efficiency is the most important factor in energy harvester systems influencing the size, weight, and cost of the system. Efficiency in energy tells us how much ambient energy is available, and what percentage of this energy we will have left to operate the devices. Particularly, in the area of implantable biomedical devices, having a small size is the key factor in being able to use harvester systems in space-limited or weight-limited areas. Decreasing the size to micro-level is favourable for implantables, but their output power is also decreased. In order to overcome these constraints, harvester interface circuits play a central role in achieving high efficiency. Thus, in the last few years there has been much effort put into minimizing the power losses between harvester and load; in other words, increasing the efficiency of harvester systems.

1.2 Energy Harvesting

Within the environment around us, there are plenty of naturally available energy sources, such as solar, thermal, wind, and mechanical. However, they are not always in a form usable as a power supply for electrical loads. Energy harvesting, also known as energy scavenging, is a term used for a system which captures or

hunts the available ambient energy, and converts it into electrical energy [1].

In this thesis, we are particularly focusing on power conditioning for an electromagnetic energy harvester. Advances in production of low-power electronic devices, such as sensor nodes, transceivers, and RFID, small-scale energy harvesters have been considered sufficient to the needs of ultra-low-power electronic devices [2].

Autonomous Energy Harvester systems are a desirable option, in terms of having long operational life, especially in those cases where the system is deployed in rural or dangerous areas. Performing maintenance and accessing the system in such areas are both difficult[3]. In the past, the life of these devices depended on life-limited batteries, whereas using harvesters as a power source made it possible to use the system infinitely, theoretically speaking. In Figure 1.1 different types of harvest-able energy sources are shown.

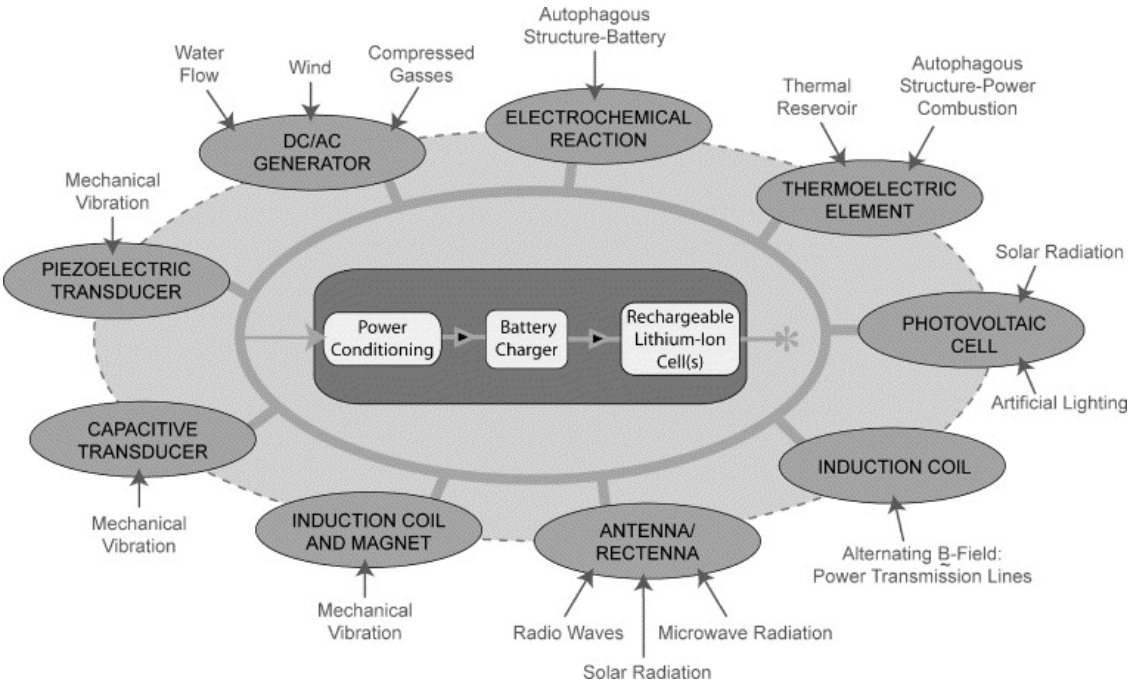

Figure 1.1: Different types of harvestable energy sources [4]

1.2.1 Energy Harvesting Basics

Energy harvesting techniques are a great option for low-power applications, as a replacement for life-constrained batteries and other energy storage devices[5]. The

output power generated by energy harvesters is usually low, however it is sufficient to supply power to wireless sensors, wearable electronics, and long-life sensors which currently have batteries or super capacitors which can need changing [6–8].

The characteristics of harvester systems differ from system to system, and a single degree of freedom lumped spring mass system is most commonly utilized to understand the dynamic behaviour of harvesters. The mechanism of energy conversion differs with each technology and the energy source used [9, 10].

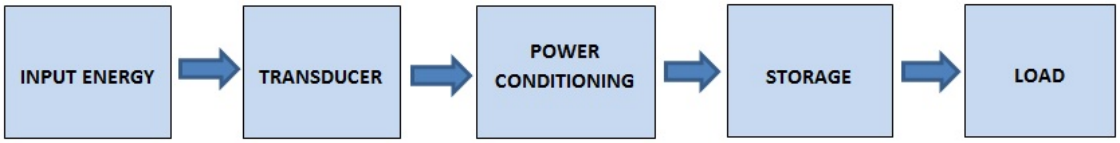

Figure 1.2: General energy harvesting system phases

Figure 1.2 shows the phases of an energy harvester system that captures ambient energy from its surroundings. The transducer is a mechanism that converts environmental energy into electrical energy using different transducer methods (e.g, electromagnetic[11], electrostatic[12], piezoelectric[13–15]). The obtained voltage and current are transient and discontinuous in nature thus, a power conditioning block is needed to form the output signal of the transducer to be able to charge the storage unit.

Usually super-capacitors and rechargeable batteries are used as energy storage units in energy harvester systems [16]. As load, sensors, signal conditioners, processors, and RF transceivers can all be considered.

1.3 Scales of Energy Harvesting

Macro-scale energy harvesting has been used for many years as an energy source. On the other hand, with the help of development in electronic devices, there are many ultra-low-power electronic devices in usage now, and it has become very common to use micro-scale energy harvesters to power such electronic devices as wireless sensor nodes, wrist watches [5, 7].

The output power of a harvester depends on many things, the size is a very important factor in the determination. Usually, the larger it is, the more power is harvested.

- Macro-Scale Energy Harvesting: generates power in a very wide range, from a few up to hundreds of watts, and has been used for many years. The power that we use in our cities, homes, and factories often comes from macro-scale energy harvesting systems through high-capacity transmission lines, which also requires distribution systems.

- Micro-Scale Energy Harvesting: generates low-level power, varying from nano-watts up to a few watts. Such harvesters have been used widely for a few decades in many different applications, including wireless sensor networks, and RFID modules [3, 17].

  Small-scale harvesters have many advantages in terms of easy design, setup, maintenance, footprint, size, cost. Micropower generators are more environmental friendly harvesters compare to macro-scale oil-based energy harvesters.On the other hand, they have disadvantages in term of discontinuity of power, power predictability, and low output power.

1.4 Types of Energy Harvesting

The relation between humanity and energy probably goes back to the beginning of human life. People need energy for many different reasons, such as heating, cooling, doing housework, or harvesting on farms. Really, it's central to every aspect of life. People have invented various methods to get energy from the environment, such as the use of watermills, windmills, and solar, all of which have been used for centuries.

Until recently, people have studied only large-scale harvesting systems, on the order of hundreds of watts output power, but with the advance of technology in producing electronic devices which can operate on milliwatts of power, researchers and scientists have begun showing interest in micro-power energy harvester systems.

Currently there are many different energy harvesting techniques using a wider variety of energy resources which are available in low amounts of power all around us.

1.4.1 Solar Energy Harvesting

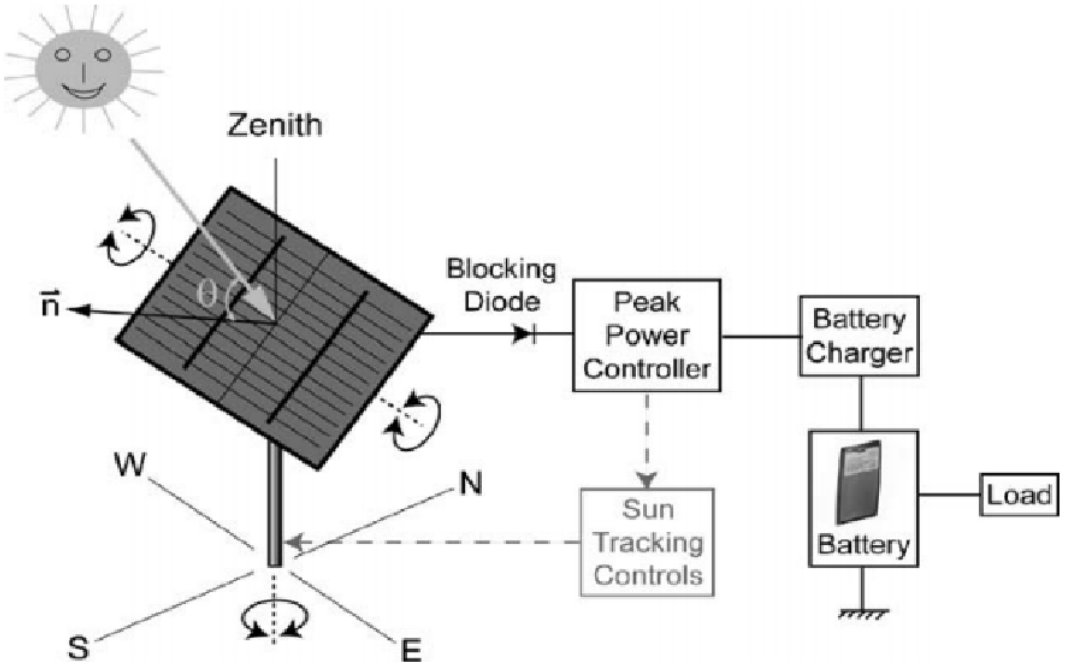

Figure 1.3: Typical solar harvester system[4]

Solar energy (solar radiation) is always naturally available on a bright sunny day outdoors and artificially available in lighted indoor environments. Solar power systems can be found generating electricity in a range from milliwatts to megawatts, for different applications: calculators, wrist watches, grid-connected PV systems. Solar power systems generally consist of low-cost PV cells, and provide enough current and voltage level to which meet the power requirements of most microelectronic circuits [9].

Recently the majority of solar cells, which convert solar energy to electrical energy by using the photovoltaic effect, are made from semi-conductor materials. Solar cells have the feature that they can be excited by solar (photon) radiation.

When a photon hits the solar cell, it causes an electron to leave an atom, and the electron starts moving through the cell, generating electricity through the photovoltaic effect.

Depending on the method used to capture, convert, and distribute the solar energy, such technologies are often classified into passive and active categories. Solar cells and solar thermal collectors are grouped as active solar energy technologies, while passive solar energy technology can include adjusting the position of a building relative to the Sun, careful selection of materials for their properties, and having building with natural air circulation.

Solar radiation amount changes over the earth's surface based on weather conditions (medium temperature, cloudy or sunny sky, blowing dust storms) and location (longitude and latitude). Approximately 1000 Wm^{-2} of solar power falls on the surface of Earth facing directly towards the Sun on a bright sunny day [18]. In any particular location there will be an optimum slope angle and orientation of the PV solar cells for obtaining the maximum solar radiation over the solar cell.

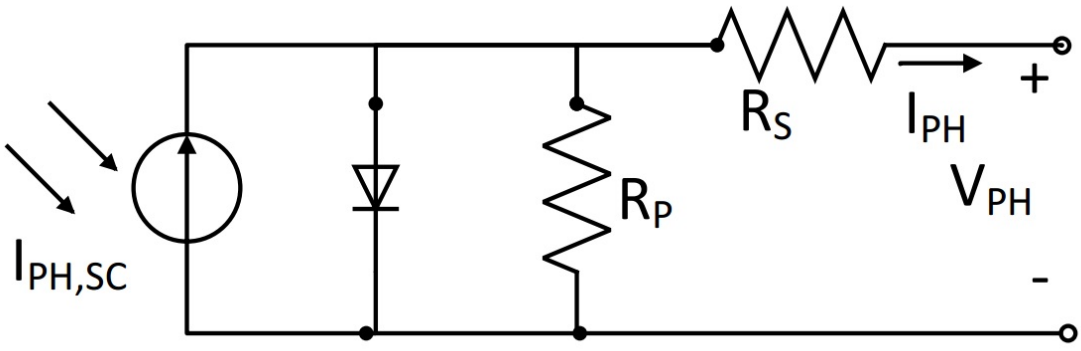

Figure 1.4: Electrical model of a PV module

Typically, commercially available PV cells have an efficiency around 15%.

A typical solar harvester system consists of a solar panel module, peak power and sun tracking control units, and a battery and battery charger, as shown in Figure 1.3 [4].

In Figure 1.4, the electrical model of a PV module is shown [19]. $I_{PH,SC}$ is

basically generated current, R_S the parasitic series resistance, and R_P the equivalent shunt resistance. At the output terminal there are I_{PH} and V_{PH} as the output current and output voltage of the PV cell respectively.

1.4.2 Thermal Energy Harvesting

Thermal energy is another type of energy source, and can be found in almost any environment.Typical examples of thermal energy source : waste heat from car exhausts, radiators, geothermal from underground, and temperature difference between the top and bottom layers of seas.

A thermoelectric generator (TEG) does not have any moving parts, and hence is quiet, reliable, scalable, and environmentally friendly; thus, TEGs have became very alluring for human body-powered biomedical devices. When a whole typical human body is used for thermal energy harvesting, the available power is 6.4 W (assuming human body temperature of 37° Celsius and ambient temperature of 20° Celsius) when using a device covering only the neck, a supply 0.2 to 0.32 W of power could be generated, while a typical human dissipates 116 W power sitting still [9].

A typical TEG consist of a thermocouple which has many p-type and n-type semi-conductor pillars, which produces an electrical current proportional to temperature difference between the hot surface (e.g., the human body) and the cold surface (e.g, ambient air), based on the Seebeck effect. The Seebeck effect is a phenomenon which produces a voltage by a temperature gradient between two surfaces. Thermocouples are generally connected in series electrically and in parallel thermally. Since using an individual thermocouple is not suitable to power many electronic devices, using multiple thermocouple arrays to increase voltage and power level is established in the literature [9].

When there is a temperature gradient (ΔT) between two surfaces made of two different conductor materials, a voltage V develops between two points as given by

$$V = \alpha_1 \Delta T - \alpha_2 \Delta T \tag{1.1}$$

where α_1 and α_2 are material-dependent Seebeck coefficients. The Seebeck coefficient is positive for p-type material used as pillars, and negative for n-type material used as pillars, so the contribution of two pillars adds up if two different dopings are used for the pillars. Figure 1.5 illustrates the working mechanism for a TEG.

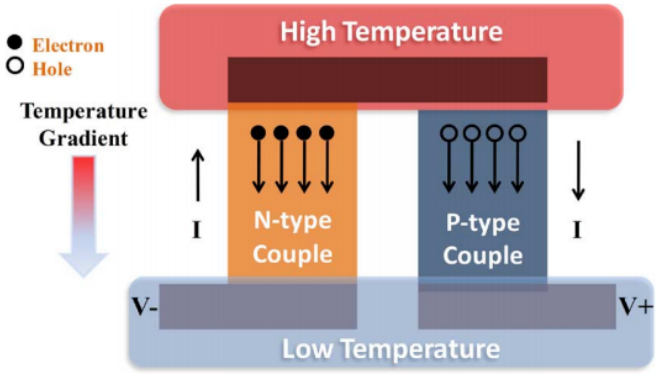

Figure 1.5: Illustration of operation mechanism of a TEG [19]

There are many companies producing commercially available TEG modules. For instance, Marlow Industries Inc., of the United States, has modules which can generate up to 8W output power from a 180K temperature gradient, while another company from Germany, Micropelt, has wireless sensor nodes with powered TEGs [1].

1.4.3 Kinetic Energy Harvesting

Kinetic energy is associated with the motion of a object, and is generally found in the environment in the form of vibrations, random displacements, or forces [1]. Vibration-based harvesting devices are typically modelled as mass m, spring with stiffness k, and damper with a viscous damping coefficient b; such systems are

shown in Figure 1.6. The seismic mass is suspended in the outer case, and the whole system moves relative to the inertial frame with the position of the case at time t described by $u(t)$. The position of the seismic mass relative to its equilibrium position in the case is $x(t)$. The damper represents the losses in the system, and the extracted energy. The equation of motion for the system may be written as

$$m\ddot{x}(t) + b\dot{x}(t) + kx(t) = -m\ddot{u}(t) \tag{1.2}$$

Assuming that the external base excitation is sinusoidal as $u(t) = U\sin(wt)$, then the steady state solution for $x(t)$ will be

$$x(t) = \frac{w^2}{\sqrt{(\frac{k}{m} - w^2)^2 + (\frac{bw}{m})^2}} U\sin(wt + \phi) \tag{1.3}$$

When the natural frequency $w_n = \sqrt{\frac{k}{m}}$ of the resonant system matches the vibration frequency ($w = w_n$), peak power occurs in the system. Vibration-powered generators employ three main transduction methods to extract mechanical energy from the system and convert it into electrical power. These transduction methods are piezoelectric, electromagnetic, and electrostatic techniques.

1.4.3.1 Piezoelectric

The piezoelectric effect was discovered by Jacques and Pierre Curie in 1880. When a certain type of materials (piezoelectric materials) undergoes a mechanical strain or deformation (structural vibration), there is a charge separation across the device, as a result producing a voltage proportional to the stress applied. This is the piezoelectric effect, which has have been used for translating mechanical energy to electrical energy for many years.

PVDF, polyvinylidene fluoride, and PZT, lead zirconate titanate are two most common piezoelectric material types, and there are three ways to excite these materials to generate electrical energy: compression, slap, and bending [20].

Piezoelectric harvesters can sorted into two categories: human-powered piezo-

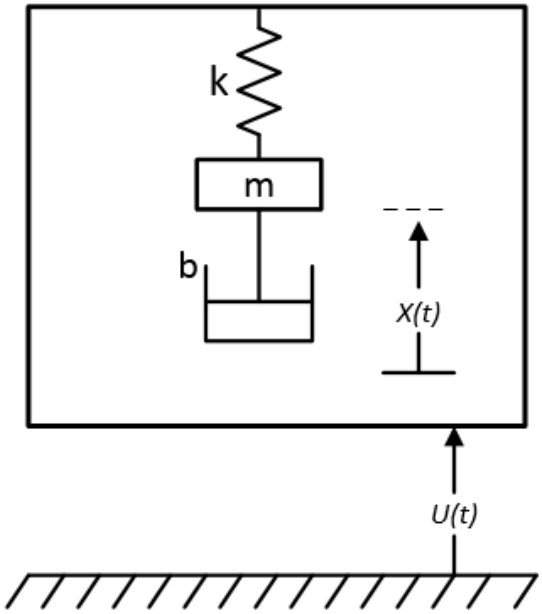

Figure 1.6: Model of a mass-spring-damper system for vibration based energy harvesters

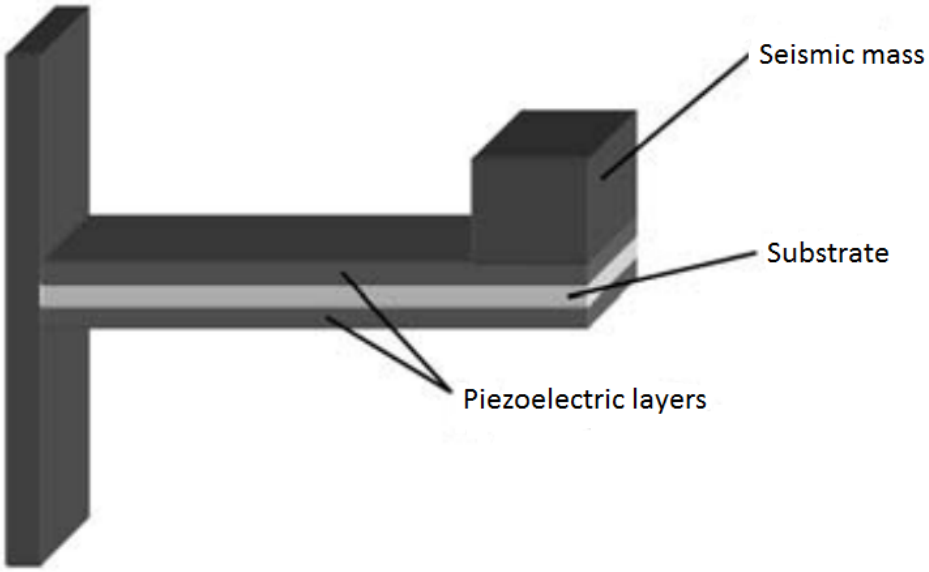

Figure 1.7: Piezoelectric cantilever beam structure generator

electric generators, and vibration-based cantilever piezoelectric generators [11].

Energy harvesting from human body motion has been studied extensively by researchers for implantable and wearable electronics. Human motion characteristi-

cally has large amplitude and low frequency; on the other hand, generally speaking the smaller the device, the higher the natural frequency. Thus it is hard to find miniaturized human-motion-based piezoelectric generators operating on the human body [11].

There are many applications of human-powered piezoelectric generators in the literature [22], [11].

Khaligh *et al* [11] showed how different human-powered scavengers, especially shoes, which have had piezoelectric materials attached to them. The shoe-mounted systems took advantage of the bending movement of the ball of the foot to generate electrical energy on the piezoelectric material. The generated power ranges from 2.3 μW to 8.4 mW, and operation frequency is about 1Hz [11].

Using cantilever beam geometry is very popular for energy harvesting from vibration. The cantilever beam can be in the form of uni-morph (only one piezoelectric layer on one of the surface), or of a bi-morph (which has two piezoelectric layers, on both surfaces, bottom and top). The cantilever structure has a low resonant frequency, which can be decreased by adding mass to the free end of the beam [11].

They have ability to produce a relatively high voltage, but usually with low current. Their output impedance is typically very high, more than 100 kΩ.

1.4.3.2 Electrostatic

The relative movement of charged (the charge is introduced from an external power source) and electrically isolated from one another plates (capacitor), or the distance change between the plates, is utilized for the electrostatic type of energy harvesting. Electrostatic generators can be labelled as either voltage- or charge-constrained type generators. In voltage-constrained type; the voltage applied to the plates is held constant, and the change in the capacitance will change the charge on the plates. In the charge-constrained type, the charge is kept constant, and the voltage will change as a result of change in capacitance. The voltage variation in the plates results in a current flowing towards the load. Both types of generator have different

characteristic advantages and disadvantages.

The charge on the plates is calculated by Equation 1.4, and the capacitance between two charged plates is calculated by Equation 1.5

$$Q = CV_o \tag{1.4}$$

$$C = \epsilon_r \epsilon_o \frac{A}{d} \tag{1.5}$$

where C is the capacitance (farads), V is the voltage (volts), Q is the charge (coulombs), A the area of the plates m^2, d is the gap between the plates (m), ϵ is the permittivity of the material which isolates the plates electrically, and ϵ_0 is the permittivity of free space ($\mathrm{F}m^{-1}$). The energy stored on the capacitor is

$$E = \frac{1}{2} QV. \tag{1.6}$$

If the type is charge-constrained, then we can rearrange the energy equation as

$$E = \frac{Q^2 d}{2\epsilon A} \tag{1.7}$$

while if the voltage is constrained, the energy becomes

$$E = \frac{\epsilon A V^2}{2d} \tag{1.8}$$

Energy density can be increased by decreasing the distance between plates, or by decreasing the plate surface area, so the major advantage of the electrostatic generators is that they are the most suitable type for micro-engineered devices. The main drawback of this type is that it needs an initial voltage (or charge) to polarize the plates. The output voltage is relatively high (greater than 100V), but as a result of having relatively high output impedance, their current is limited.

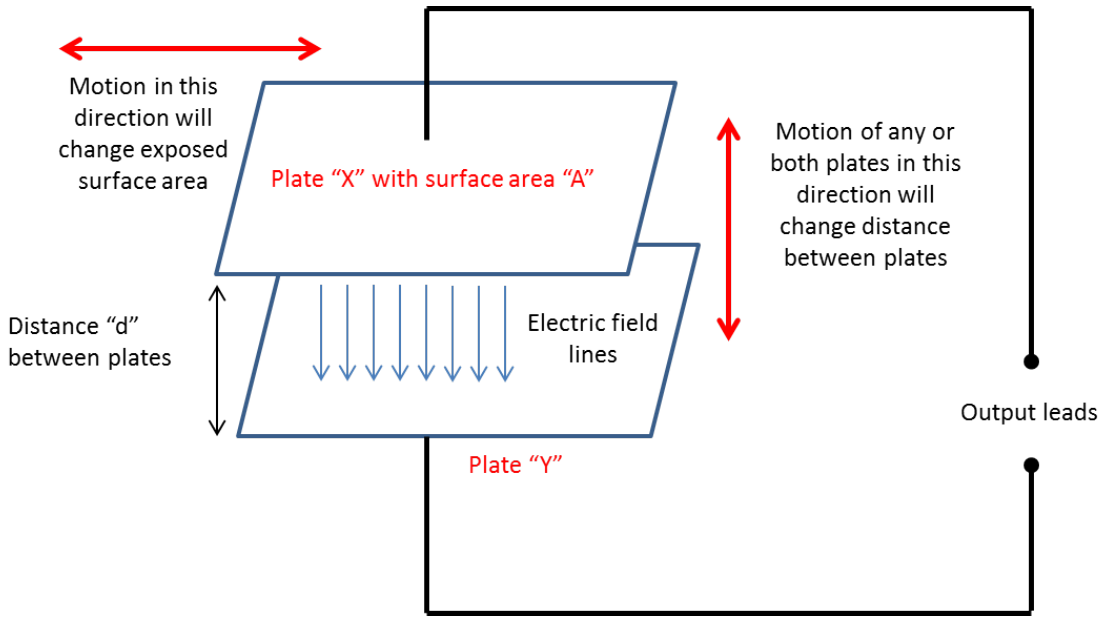

Figure 1.8: A typical electrostatic energy harvest [23]

1.4.3.3 Electromagnetic

Electromagnetic energy generators utilize Faraday's law of electromagnetic induction to convert mechanical energy to electrical energy. According to Faraday's induction law, when a conductive coil passes through a magnetic field which is established by a stationary magnet, this causes a change in magnetic flux ϕ_m. The flux change can be utilized with either a moving coil between fixed magnets, or moving magnets around a fixed coil. The change in the magnetic flux develops a potential difference between the coil's terminals, and when a load is connected to the terminals, current will flow through the load. The voltage generated across the conductive coil V is proportional to the change of magnetic flux ϕ_m, as seen below.

$$V = -\frac{d\phi}{dt} \tag{1.9}$$

The induced voltage for a single coil turn is relatively small, so in order to make the generator a reliable source of energy, there are possible techniques: increase the number of coil turns; increase the size of magnets to get bigger magnetic field; or use a transformer to increase the output voltage.

When a coil is used with N turns, the voltage obtained will be as Equation 1.7.

$$V = -N\frac{d\phi}{dt} \tag{1.10}$$

As kinetic energy is used as an external force to create the motion of coil or magnets, the output voltage can be expressed as

$$V = -N\frac{d\phi}{dt}\frac{dx}{dt} \tag{1.11}$$

where $\frac{dx}{dt}$ is the rate of change of relative displacement, the velocity of motion in the x-direction.

1.5 Thesis Outline

In Chapter One, we explored basics of Energy Harvesting Systems (EHS). We also covered EHSs based on their scale and transducer types.W e gave technical background information about three common energy harvesting types and their working principles.

In Chapter Two, we will discuss the basics of power management in EHS, and particularly in vibration-based energy harvesters. We will talk about the Maximum Power Transfer Theorem, and how this theorem could be applied in EHSs. We will also introduce AC-DC rectification and types, and the basic circuit elements used in rectification circuits.

In the third chapter, we will introduce MOSFETs and types, and discuss passive and active full-wave AC-DC rectification realized with discrete MOSFET circuit elements. We also built the passive full-wave MOSFET rectifier on breadboard, and tested it with a function generator.

In the last chapter, we will show how we tested our rectifier with EMH for different cases, and explore the effect of the rectifier on the harvester and its performance.

In the conclusion, we conclude our results and talk about future potential work

about rectification in harvesters.

Chapter 2

Power Management in Vibration-Based Energy Harvesters

2.1 Power Conditioning

Environmentally available mechanical energy can be harvested using a suitable energy transducer mechanism, such as electromagnetic, electrostatic, or piezoelectric. These vibration-based energy generators convert the mechanical vibration energy into AC electrical energy, however in order to power many electronic devices, there is a need for stable DC electrical power. Typically, to supply DC power to an electrical load, first the raw mechanical energy has to be captured from environment and converted into AC electrical power. Once we get AC power, it has to be processed by a power conditioning circuit, to make it suitable DC power to energize electrical loads. These steps are illustrated in Figure 2.1.

The losses are a serious issue in harvester systems because of the limited output power we have out of harvesters. There are two main types of loss in the system; one of these is mechanical loss from mechanical damping, and the other is electrical loss from power consumption of conditioner electronic devices.

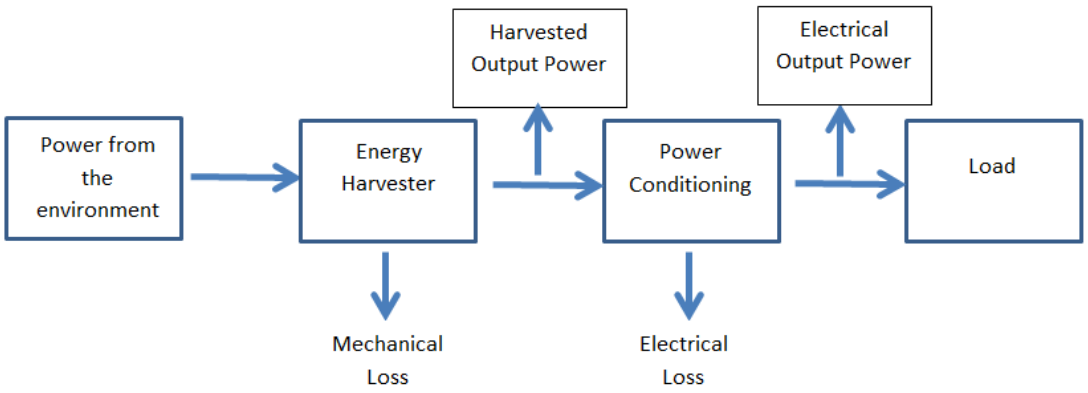

Figure 2.1: Power flow from environment to electronic load

2.2 Maximum Power Transfer Theorem in Harvesters

Maximum Power Transfer Theorem explains what the criteria are to deliver the source power to the electrical load with maximum transfer efficiency. Maximum power transfer occurs when the source impedance of an AC source is the complex conjugate of load impedance [24].

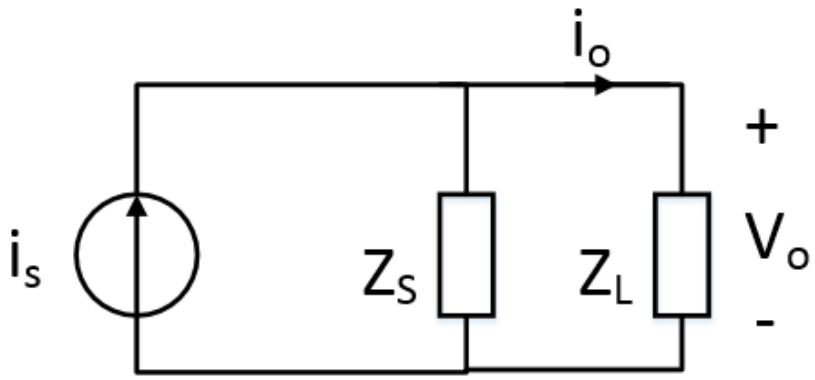

Figure 2.2: The circuit with an AC current source

Consider the AC current source shown in Figure 2.2, with an internal impedance $Z_S = R_S + jX_S$ and a load impedance of $Z_L = R_L + jX_L$. To deliver maximum

power from the mechanical side to the electrical load, the load impedance should be the complex conjugate of Z_S, $Z_L = R_L - jX_S$. Maximum power is then derived by

$$P_{max} = \frac{R_S^2 + X_S^2}{4R_S} I_S^2 \tag{2.1}$$

where R_S is the internal resistance of the power source.

The same maximum power relation can be drawn for a voltage source of $v_s(t) = \sqrt{2}V_s sin(\omega(t))$ as shown in Figure 2.3, as given in Equation 2.2.

$$P_{max} = \frac{V_S^2}{4R_S} \tag{2.2}$$

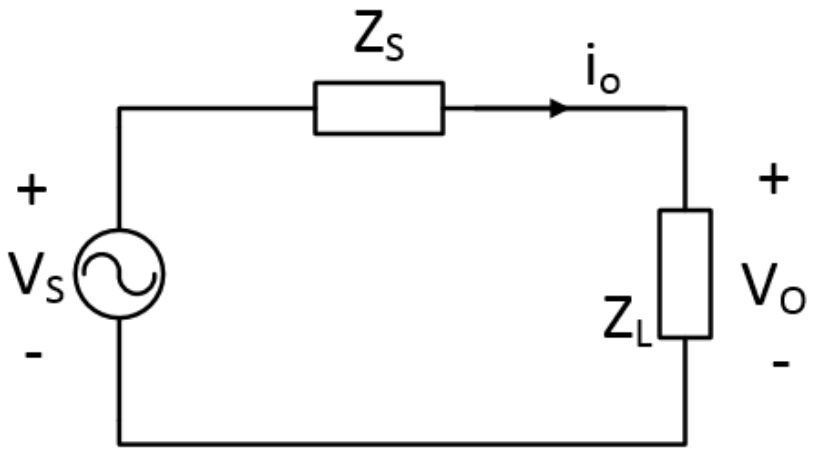

Figure 2.3: The circuit with an AC voltage source

Power transfer from an energy harvester is highly affected by the load impedance which is connected to the harvester. In order to minimize power loss due to mismatching of impedances between harvester and interface circuitry, there is the impedance matching technique. Impedance matching is also the technique able to deliver maximum power from the harvester to the electrical side there have been various impedance matching techniques in the literature [30, 31]. There are two well-known impedance matching techniques, known as resistive impedance matching and complex conjugate impedance matching [24]. Proynov *et.al* in [31] managed impedance matching between the input impedance of the converter and the output

impedance of the source, by changing the duty ratio D dynamically.

2.3 Common Components Used in Rectification

There are basic and fundamental components in rectification, such as diodes, transformers, and capacitors. In this section we will give basic information about these devices.

2.3.1 Diodes

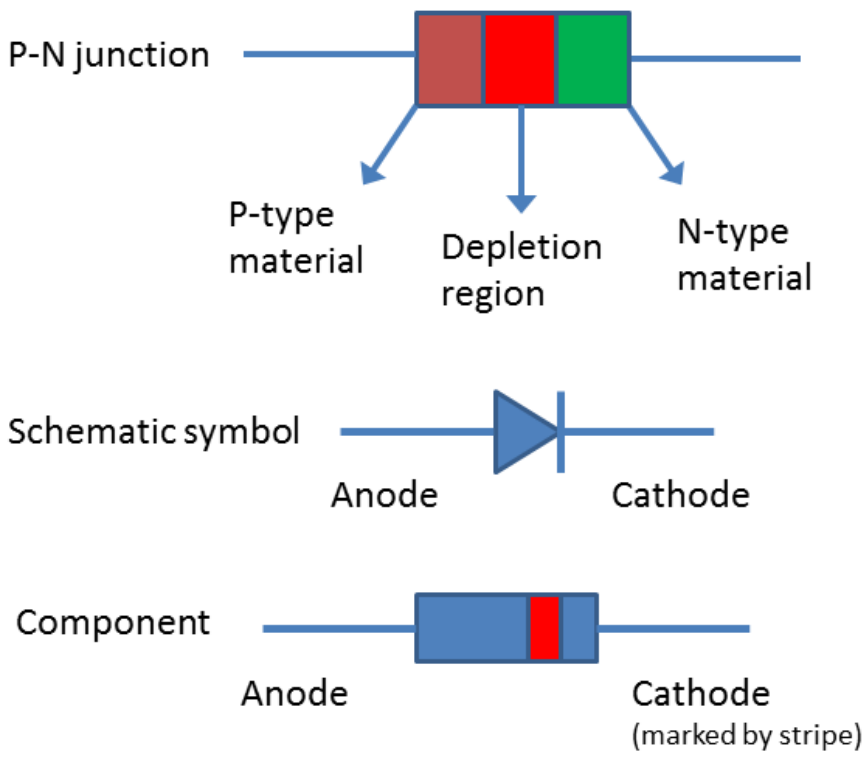

Figure 2.4: Representation of a semiconductor diode

The diode is the simplest and most fundamental non-linear circuit element, which has a non-linear $i - v$ characteristic, unlike the resistor. It is a two-terminal circuit element with a circuit symbol shown in Figure 2.4, and the $i-v$ characteristic shown in Figure 2.5.

An ideal diode has the characteristic of allowing current to pass through it only in one direction, while blocking the current in the reverse direction. The diode may be thought as a kind of switch: "closed" when forward-biased (anode terminal voltage higher than cathode terminal voltage), and "open" when reverse-biased (cathode terminal voltage higher than anode terminal voltage).

However in reality, the diode has the $i - v$ characteristic shown in Figure 2.5. It allows current to pass through it when the forward voltage is equal to or higher than the required minimum voltage. On the other side, the diode does not block the current flow forever when it is reverse-biased. When the applied voltage exceeds some certain voltage value, called the reverse breakdown voltage, V_Z in reverse direction, current starts to pass through the diode in the reverse direction, as seen in Figure 2.5.

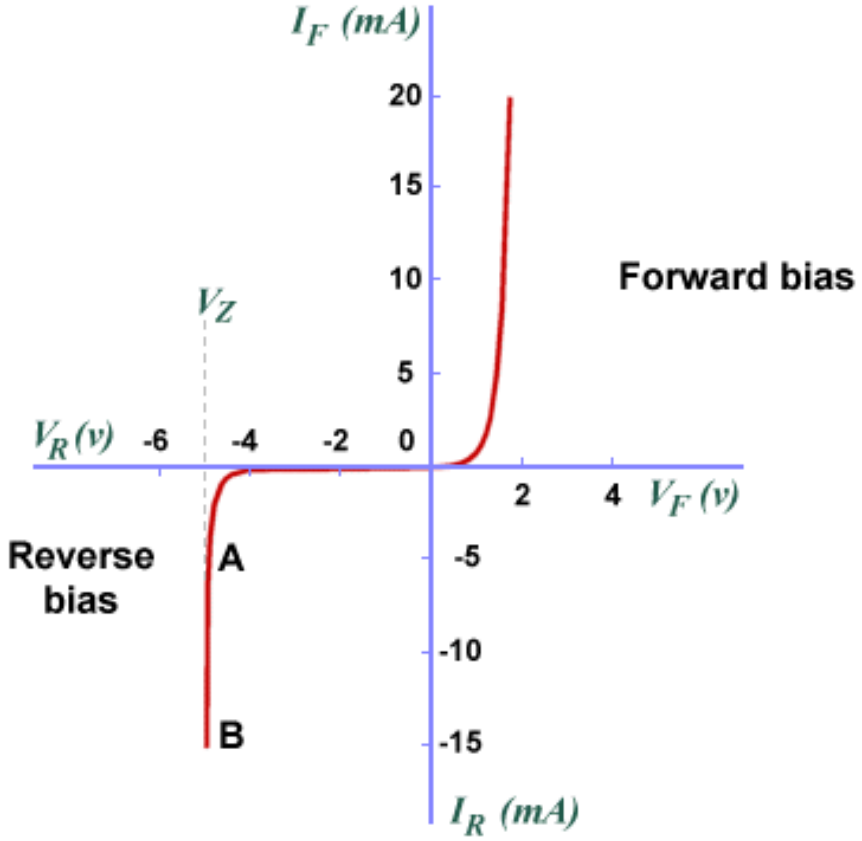

Figure 2.5: $i - v$ characteristic of a diode

When the diode is forward-biased and allows current through it, there will be a voltage drop across it, because of the depletion region formed by the P-N junction. The depletion region usually has a small number of charge carriers, so it acts as an insulator in normal conditions. When the diode is forward-biased, there is a need to have a certain voltage level (known as forward voltage, V_f) to collapse the depletion region fully and eliminate the barrier against current flow. Forward voltage changes based on the chemical properties of the P-N junction; for example, for a silicon diode, the typical forward voltage is 0.7V, while for germanium diodes, it is 0.3V and for Schottky diodes it even goes down to 0.1V.

2.3.2 Transformers

A transformer is a static device that converts electrical power in an AC system from one voltage or current level to another. It deploys the principle of magnetic induction between coils without using any rotating parts. A transformer usually consists of three parts, as seen in Figure 2.6: the primary coil, which is connected to a supply source; the core, made of ferromagnetic material; and the secondary winding, which delivers power to the load. However sometimes there is a kind of transformer that has only one winding, which serves the dual purpose of both primary and secondary coils.

The primary winding is connected to an AC power source and carries the AC current this may be either the high- or low-voltage winding, depending on the application. The secondary winding is the side which is connected to the load. It, too, may be either the high- or low-voltage winding, depending on the application.

The core is the place where the varying primary current creates varying magnetic flux over it. This varying magnetic flux induces a varying electro-motor force, or voltage, in the secondary winding.

Transformers can be classified based on different criteria, such as method of cooling, insulation between windings, number of phases, method of mounting, purpose of usage, *etc.* In general we can classify them into two groups: the $step-up\ transformer$, in which the secondary winding voltage is greater than the primary

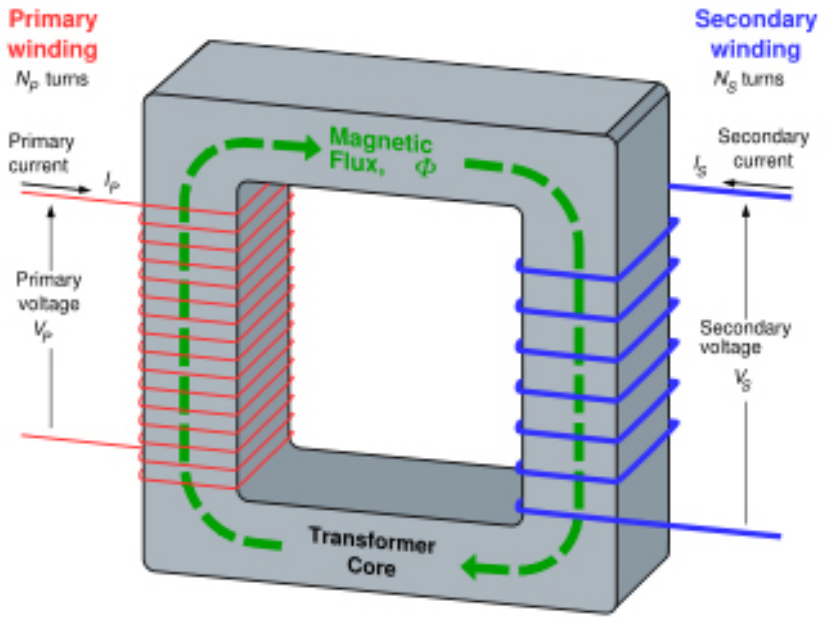

Figure 2.6: Basic transformer structure and windings [23]

winding voltage; and the *step−down transformer*, in which the secondary winding voltage is smaller than the primary winding voltage.

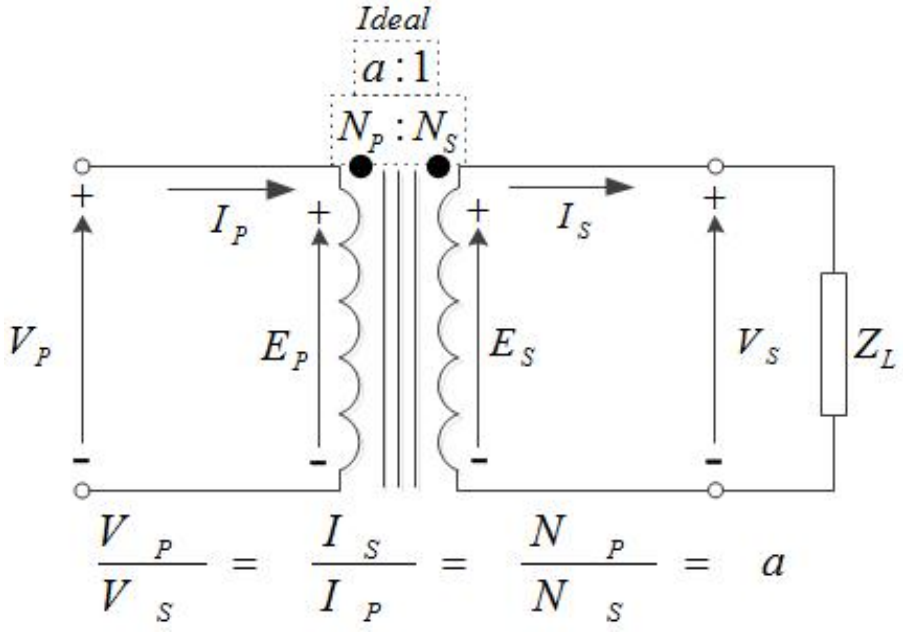

Figure 2.7: Ideal transformer circuit diagram [34]

In Figure 2.7, an ideal and perfectly coupled transformer circuit diagram is

shown, which has a proportion between primary and secondary winding voltages called voltage ratio, as defined by:

$$\frac{V_P}{V_S} = \frac{N_P}{N_S} = \alpha \tag{2.3}$$

where N_P is a primary winding turn, and N_S is a secondary winding turn.

2.3.3 Capacitors

A capacitor is a passive electrical energy storage device. Basically they consist of two conductive plates and one non-conductive layer (dielectric material) between them, as shown in Figure 2.8.

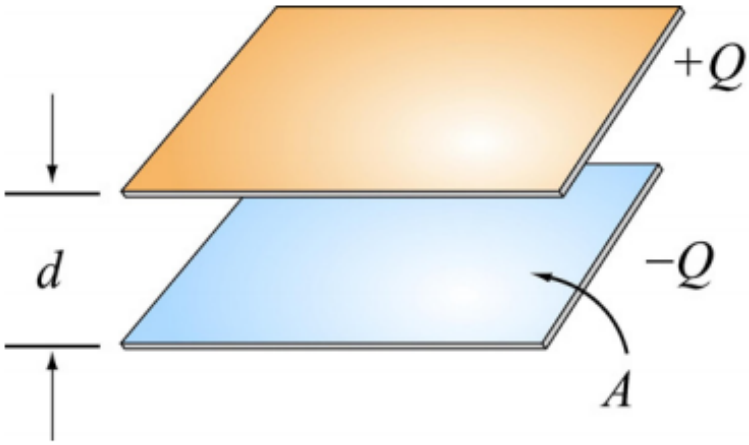

Figure 2.8: Parallel plate capacitor structure

Electric charge accumulation on one of the conductor plates induce the same amount of charge with the opposite polarity on the other conductor plate. As a result, an electric field and potential difference exists between these two plates.

Capacitance, $C = Q/V$ (SI unit of capacitance is the *Farad* (F)), is the ratio between accumulated charge on the plate and potential difference between plates; physically, capacitance can be interpreted as the electric charge storage capacity of a capacitor at a given potential difference V. On the other hand, the simple

theoretical expression of the capacitance is:

$$C = \frac{\epsilon_r \epsilon_0 A}{d} \tag{2.4}$$

where;

A=Plate area m^2

d=distance between plates m

ϵ_0=permittivity of free space $(8.854x10^{-12}F/m)$

ϵ_r=relative permittivity of the dielectric between the plates

2.4 AC-DC Conversion

Rectification is a process used to convert alternating current (AC), which periodically reverses direction, to direct current (DC), which flows in only one direction. The reason we need rectification in electronics is that most low-power electronic devices use only a low DC voltage to operate. Therefore the AC voltage obtained from harvesters needs to be rectified, converted into a usable DC voltage to supply power to the electrical loads.

Rectifier circuits are the most common diode applications in getting DC power supplies from AC power generators. The rectification types which will be discussed here are only for single-phase systems. Three-phase or multiple phase rectification systems are outside the scope of this thesis.

2.4.1 Passive and Active AC-DC Conversion

Rectification is categorized into passive and active rectification, based on the devices used, and the need for an external DC power supply. In passive rectification, passive filtering devices and diodes are usually used, while in active rectification, MOSFETs and BJTs are generally used as switches, and to control them there is a need for active drive circuits, or control circuits. Therefore, to run the active components there is a need for a DC power supply, which is usually external.

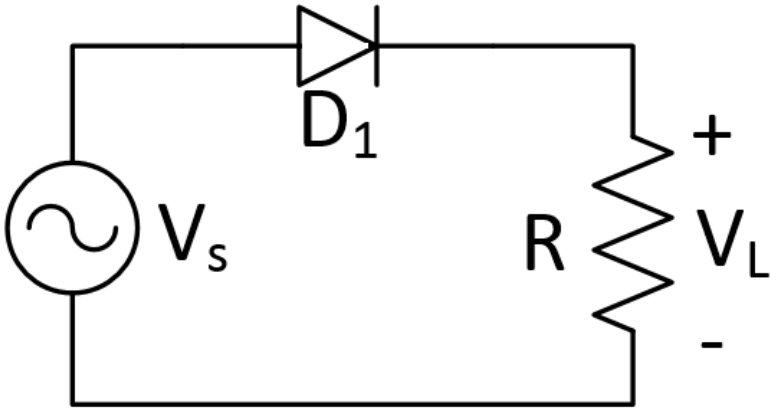

Figure 2.9: Half wave rectifier circuit diagram

2.4.2 Half-Wave Rectifier

The half-wave rectifier utilizes only a half cycle of the input sinusoidal signal, and consists of only one diode, as shown in Figure 2.10. If the diode is assumed to be an ideal diode, which has zero forward voltage drop and zero series internal resistance, the relation between input voltage V_{in} and output voltage V_{out} is as follows

$$V_{in} = V_{out} \tag{2.5}$$

The output signal in the ideal diode case overlaps the input signal, as shown in Figure 2.10(a). However, when we consider diodes in a more realistic model, which consists of an ideal diode, with forward voltage drop V_d, and internal series resistance of the diode of R_d, we obtain the output voltage shown in Figure 2.10(b). There is a voltage difference between input and output voltages due to both forward voltage drop V_d and power losses. The output voltage equation can be drawn as:

$$V_{out} = \frac{R}{R + R_d}(V_{in} - V_d) \tag{2.6}$$

in many applications, R_d is small enough to be neglected and the output voltage is

$$V_{out} \cong V_{in} - V_d \tag{2.7}$$

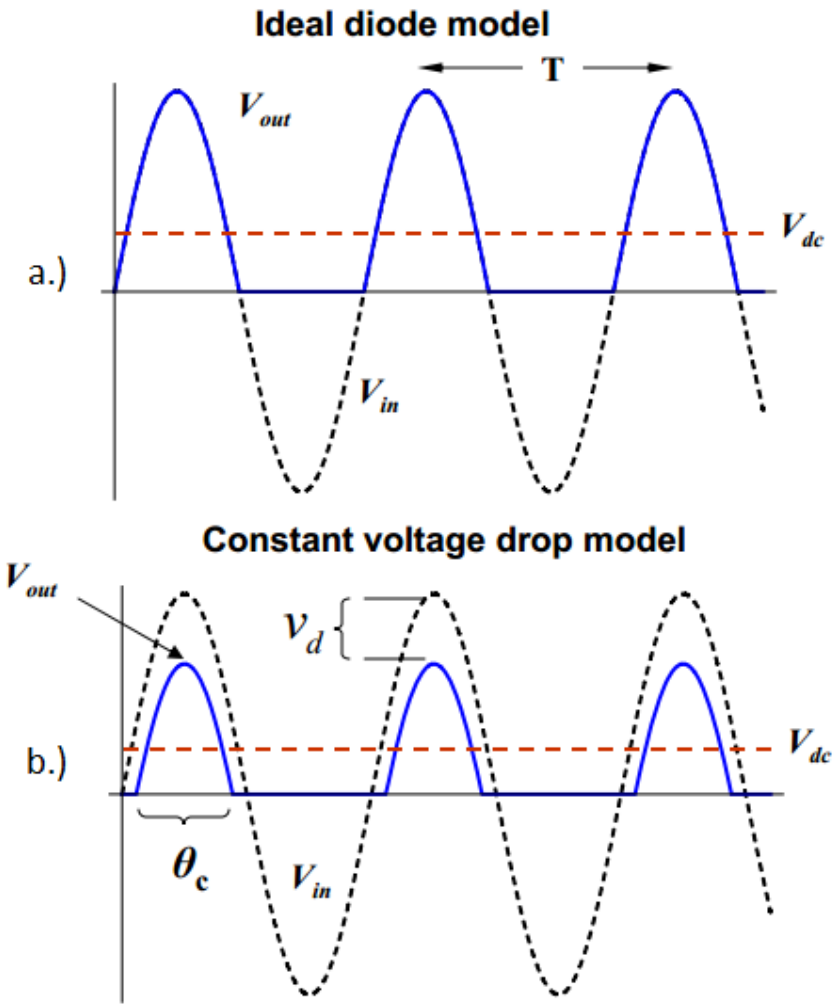

Figure 2.10: Half wave rectifier outputs a) ideal diode condition, b) real diode condition [32]

where V_d is 0.7V-1.1V for silicon diodes, 0.3V for germanium diodes, and Schottky diodes might even have a 0.2V forward voltage drop. The V_{dc} is the average DC component of the output voltage, and can be calculated as follows:

$$V_{dc} = \frac{1}{T}\int_0^T V(t)\,dt = \frac{V_{in}}{\pi} \tag{2.8}$$

where T is the period of the sinusoidal input signal. And, similarly,we can calculate

the RMS value of the output voltage:

$$V_{rms} = \sqrt{\frac{1}{T}\int_0^T V(t)^2\,dt} = \frac{V_{in}}{2} \tag{2.9}$$

The rectification ratio (η) can be calculated as

$$\eta = \frac{P_{DC}}{P_{rms} + P_{loss}} \tag{2.10}$$

$$P_{DC} = V_{DC} I_{DC} \tag{2.11}$$

$$P_{rms} = V_{rms} I_{rms} \tag{2.12}$$

$$P_{loss} = I_{rms}^2 R_d \tag{2.13}$$

If we assume ideal switches with no loss, $P_{loss} = 0$, the rectification efficiency will be

$$\eta = \frac{V_{DC}^2}{V_{rms}^2} \tag{2.14}$$

and for half-wave rectification

$$\eta = \frac{V_{DC}^2}{V_{rms}^2} = \frac{4}{\pi^2} = 0.405 \tag{2.15}$$

2.4.3 Full-Wave Rectifiers

A full-wave rectifier converts both polarities of AC input into DC output. It is generally realized by either using a center-tap transformer and two diodes, or using four diodes in a bridge configuration.

2.4.3.1 Full-Wave Center-Tapped Transformer Rectifier

In order to use both halves of an AC input voltage waveform, a full-wave rectifier with a center-tapped transformer can be used as shown in Figure 2.11. Each diode and associated half of the transformer acts like a half-wave rectifier, and the output

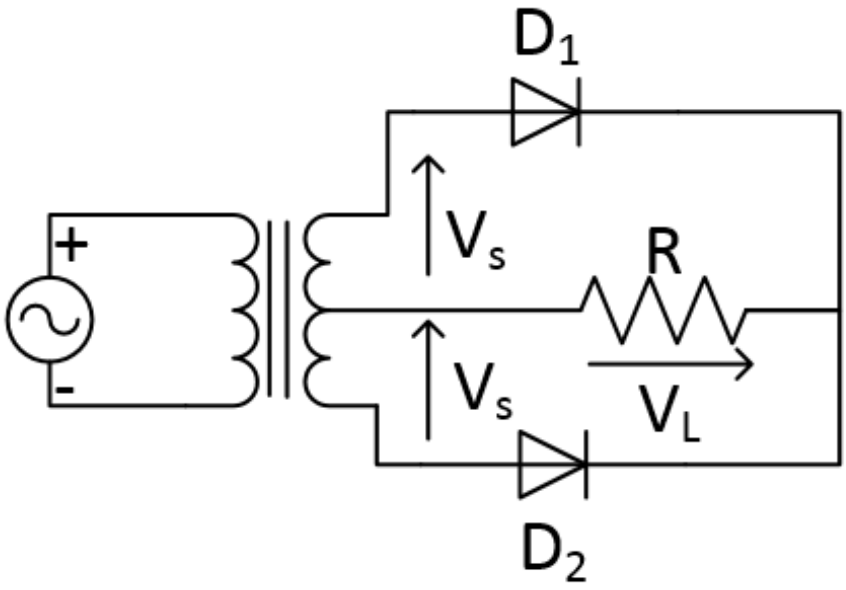

Figure 2.11: Full-wave center-tapped transformer rectifier

signal of the system is the combination of these two half-wave rectifiers' output signals, as shown in Figure 2.12. DC output voltage across the resistor for a lossless system is

$$V_{dc} = \frac{2V_{in}}{\pi} = 0.637V_{in} = 0.9V_{rms} \tag{2.16}$$

The drawback of this type is the need for a bulky transformer.

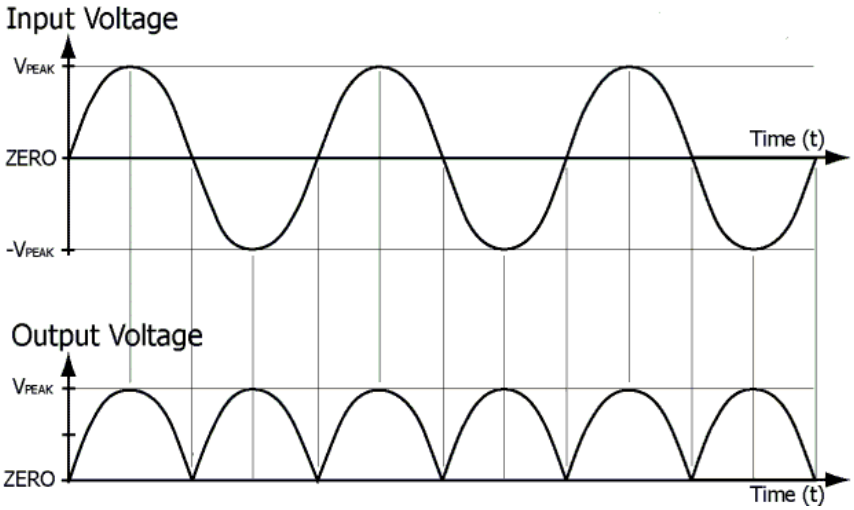

Figure 2.12: AC input and rectified output wave forms of full-wave rectifier

Using the definitions reported in the previous section, we can get similar results

for the full-wave rectification as well. If we assume ideal switches with no loss, $P_{loss} = 0$, the rectification efficiency will be:

$$\eta = \frac{V_{DC}^2}{V_{rms}^2} = 0.81 \tag{2.17}$$

2.4.3.2 Full-Wave Bridge Rectifier

Another type of full-wave rectifier is the full-wave bridge rectifier, which makes use of four diodes in a bridge arrangement, as shown in Figure 2.13. The diodes work in pairs here, and thereby the output voltage will be lowered by twice the diode forward voltage drop, $2V_d$, or approximately 1V for silicon diodes.

The main advantage this type has over the center-tapped transformer rectifier is that it does not require any transformer, thereby reducing the total size and cost of the rectifier as well.

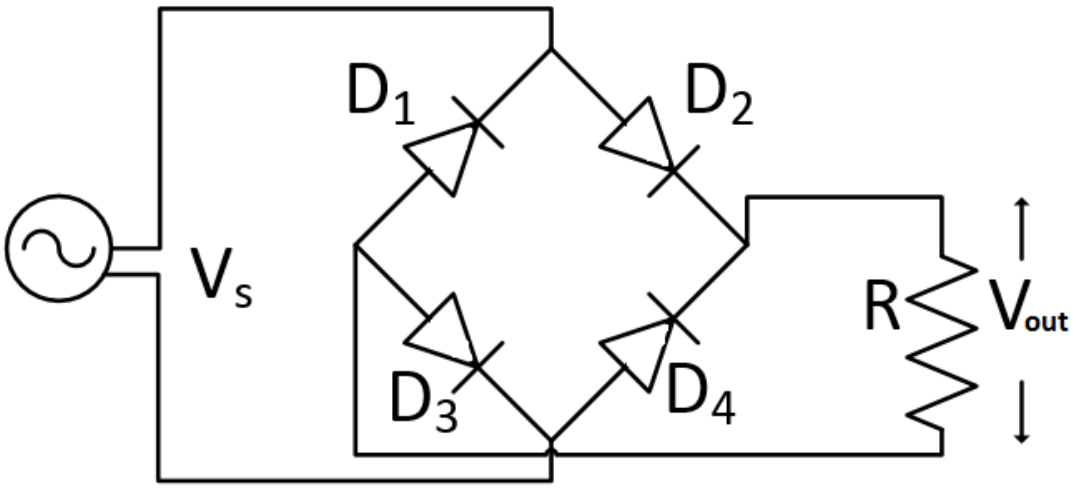

Figure 2.13: Full-wave bridge rectifier

For each cycle, only two diodes conduct the current; during the positive half cycle of the AC input, D2 and D3 are forward biased and conduct the current, while D1 and D4 are reverse biased and not conducting. However, during the negative half-cycle of the AC supply voltage, D1 and D4 are forward-biased and conduct the current, while D2 and D3 are reverse-biased and not conducting. For each case the

direction of the current is the same, so we have unidirectional current flow, which is DC voltage.

2.4.4 The Smoothing Capacitor

If we try to use the full-wave rectifier output as a DC power supply, it will cause problems with the circuits because of the huge fluctuation in the wave-form. In addition to eliminating the ripples, it is also possible to increase the V_{dc} even higher by using a parallel smoothing capacitor before the load, as shown in Figure 2.14.

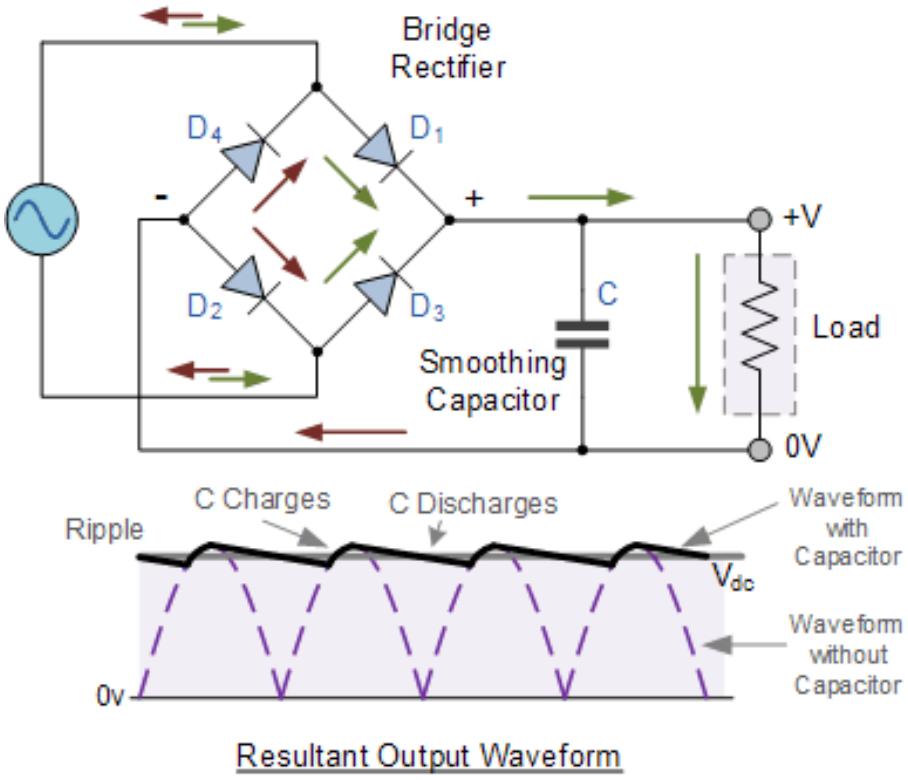

Figure 2.14: Full-wave bridge rectifier [35]

Chapter 3

Implementing MOSFET Rectifiers

3.1 Introduction

Conventional passive full-wave bridge rectification has four junction-based diodes (p/n or Schottky). Junction-based diodes are not the best option for micro-harvesters, which have low-voltage output, because of their forward voltage drop V_d of at least 0.2V. Since the voltage drop across the diodes is relatively high, compared to the output voltage of micro-harvesters, this voltage drop results in poor voltage efficiency in rectification. For instance, in case of trying to rectify a 1V AC signal with Schottky diodes (minimum 0.1V voltage drop) will cause at least 20% power loss.

To eliminate forward voltage drop across the diodes and power loss in the diode-biased full-wave rectifiers, there is a new type of full-wave rectifier which uses four MOSFETs in a bridge configuration [27]; two P-type and two N-type MOSFETs. MOSFETs act as a switch with a small on-resistance when they are fully turned on. To turn the MOSFETs on, there is a threshold voltage that which must be applied to the gate of the MOSFET, which determines the minimum voltage requirement to start operation of a MOSFET.

3.2 Types of MOSFETs

All MOSFETs (Metal Oxide Semiconductor Field Effect Transistor) are a type of Field Effect Transistor (FET) that consist of metal (M), SiO_2 (oxide or O) and Si(S). The idea behind the MOSFET operation is to control the source-to-drain current by controlling the gate voltage. In other word we cay say it is voltage controlled current source.

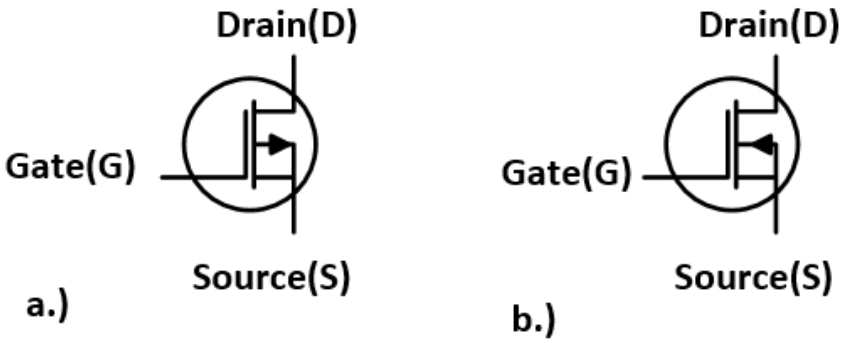

Figure 3.1: MOSFET types; a)P-type MOSFET, b) N-type MOSFET

There are two types of MOSFET, distinguished by the doping material on the wafer; P-channel or N-channel as shown in Figure 3.1. In order to understand the full operation characteristic of the MOSFETs I-V, characteristic curves are shown in Figure 3.2.

For both MOSFET types there is a required voltage V_{GS}, which has to be applied to the gate of the MOSFETs to charge the gate capacitor of the MOSFET. This necessary voltage to the gate, known as threshold voltage (V_{th}), forms a conduction channel between source and drain, which is the path of drain current (I_D). Threshold voltage is positive for N-channel, and negative for P-channel, types of MOSFET.

The MOSFET operation can be assigned to three regions, based on voltage at the terminals; the OFF state cut-off region $V_{GS}<V_{th}$; the triode region $V_{GS}>V_{th}$ and $V_{DS}<V_{GS}-V_{th}$; and the ON state saturation-region, where $V_{GS}>V_{th}$; and the $V_{DS}\geq V_{GS}-V_{th}$.

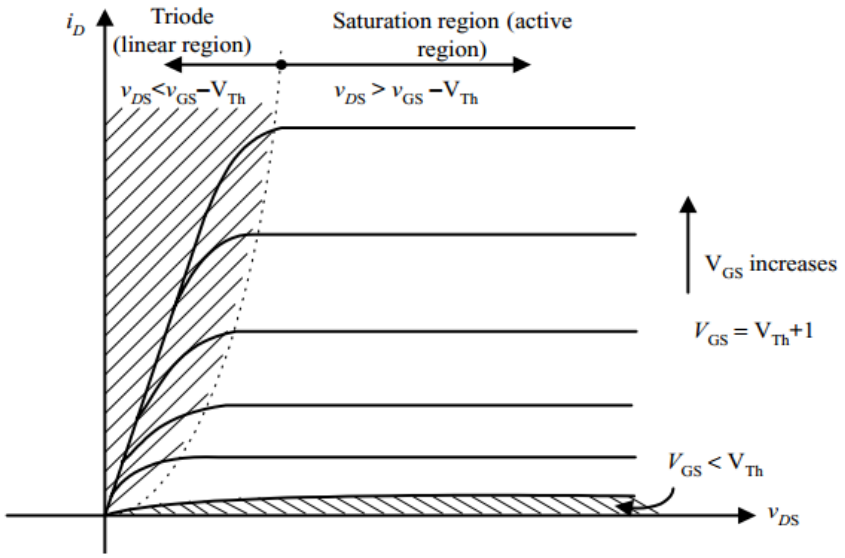

Figure 3.2: MOSFET characteristic I-V curves [33]

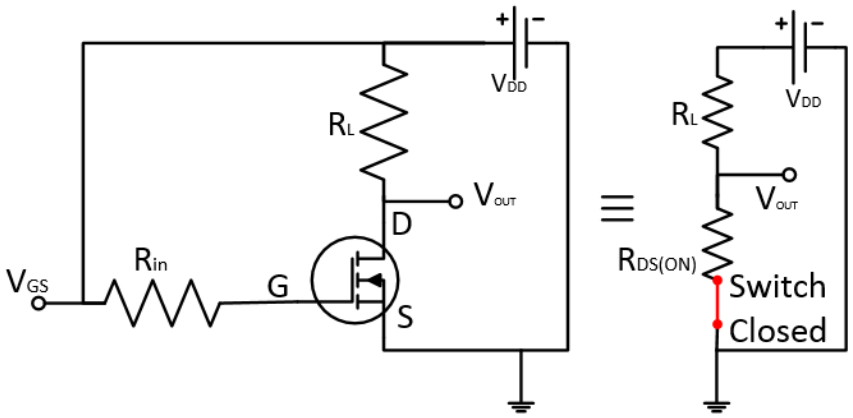

Figure 3.3: Saturation region characteristic

As the gate voltage (V_G) increases above the threshold voltage, the MOSFET starts conducting, and the current is related to the on-resistance ($R_{DS(on)}$) and the voltage applied to the drain V_D, as defined by:

$$R_{DS(on)} = \frac{V_D}{I_D} \tag{3.1}$$

In order to turn the MOSFET fully on, there must be sufficient V_G, and when the gate voltage is high, conversely the $R_{DS(on)}$ will be small.

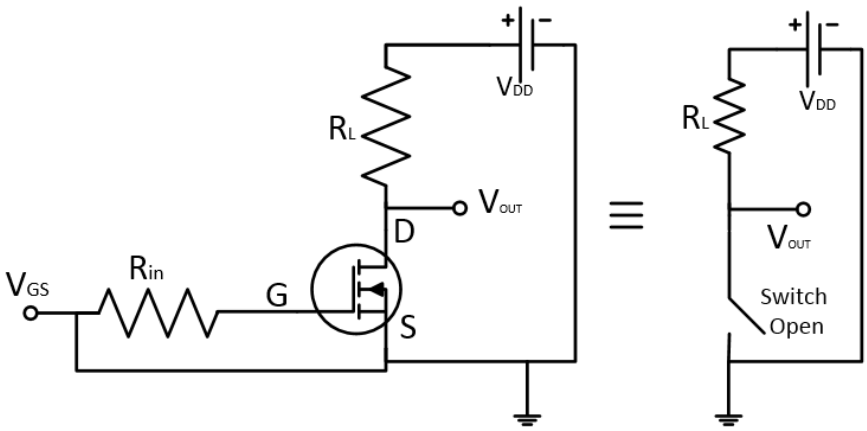

Figure 3.4: MOSFET cut-off characteristic

The parasitic capacitances between the MOSFET's three terminals affect the switching behaviour of the MOSFETs. These capacitances are gate-to-source (C_{GS}), gate-to-drain (C_{GD}), and drain-to-source (C_{DS}), as shown in Figure 3.5. These capacitances' values are non-linear, and are a function of device structure, geometry, and bias voltages.

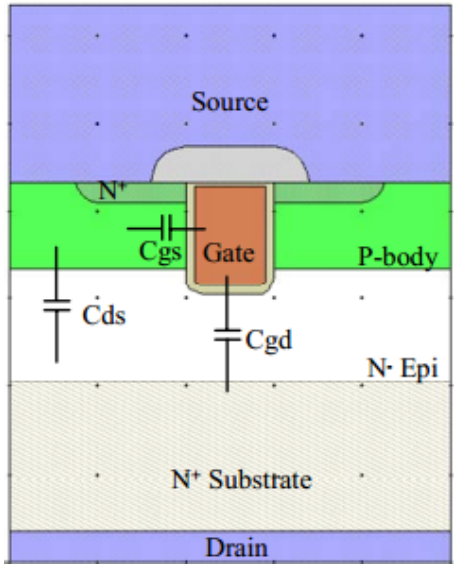

Figure 3.5: Illustration of MOSFET parasitic capacitances

Gate charge (Q_G) can be used to estimate the switching times of the MOSFET once the gate current is known.

3.3 Passive Full-Wave MOSFET Rectifiers

Conventional rectifier circuits are composed of either four or two diodes for full-wave and half-wave rectifiers, respectively. The simplest way to realize full-wave bridge rectification is to use four silicon diodes in a bridge configuration. Even though a full-wave rectifier offers a higher power efficiency, smaller output ripples, and greater breakdown voltage compared to half-wave rectifiers, their most serious drawback in the case of micro-power generators is a significant forward voltage drop when the device is conducting in the forward direction, and leakage current when the diode is reverse biased. In particular, the forward voltage drop results in undesirable voltage and power losses, and reduces the total system efficiency.

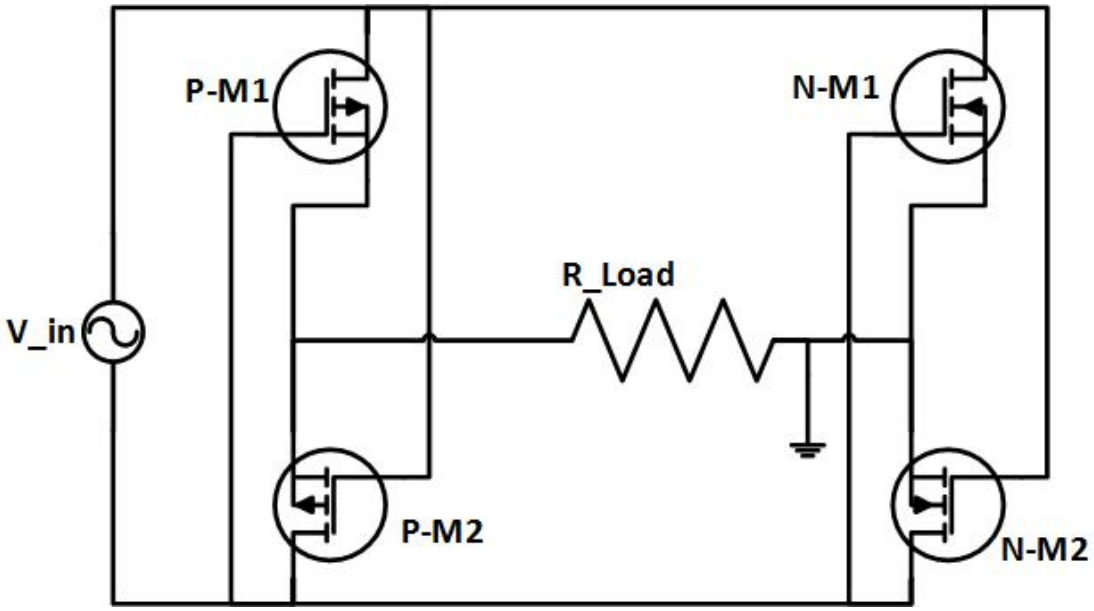

Figure 3.6: Full-wave passive MOSFET rectifier circuit

To minimize forward voltage drop, many different circuit topologies have been studied [21, 26]. Recently, integrated circuits fabricated with CMOS technology have been used to minimize voltage drop as much as possible [27, 28].

Diodes are usually replaced with MOSFETs fabricated with CMOS technology in a diode-tied configuration. Although Schottky diodes actually have a lower forward voltage drop, they have higher reverse leakage current when they are reverse-biased. In addition to having high reverse leakage current, their fabrication costs

are also high, as they are not compatible with CMOS technology [28].

In our full-wave MOSFET rectifier we used four discrete MOSFETs: two P-channel (P-M1, P-M2) and two N-channel (N-M1,N-M2) MOSFET, as seen in Figure 3.6.

MOSFETs are used as switches; P-M1 and N-M2 turn on during the positive half-cycle of the input voltage. The current follows the path starting from V_{in} over P-M1, R_{Load}, N-M2, and reaches the starting point V_{in} again. Similarly during the negative half-cycle, P-M2 and N-M1 turn ON, conduct the current to the load, and return it to the V_{in} starting point.

The critical issue in this configuration is ensuring the MOSFETs start conduction when they are supposed to. In active MOSFET rectifiers, comparators and MOSFET drivers are usually used to ensure that the MOSFETs fully turn ON and OFF at the right times. However, increasing the number of components requires more space and DC power supply to energize the active devices. On the other hand, in the passive MOSFET rectification we do not use any of these active components, rather using V_{in} as a gate drive voltage to turn the MOSFETs ON and OFF.

Usually, the silicon diodes require a minimum of 0.7V to turn on and start conduction, which adds a requirement for a step-up transformer in many micro-harvester systems. In the passive full-wave MOSFET rectifier, in addition to having low ON resistance $R_{DS(on)}$, MOSFETs have lower threshold voltages than diodes. The difference between a full-wave diode bridge rectifier and a full-wave passive MOSFET rectifier is that, instead of using four passive discrete diode elements, we use four passive discrete MOSFET elements, as seen on the breadboard Figure 3.7. As a result, we can either get rid of the bulky transformer or decrease its turns ratio of the, thereby decreasing the transformer size and thus, the total harvester system size.

The main sources of power loss in MOSFETs are during switching transition (known as switching loss) and during the ON- and OFF-states (known as conduction loss). When the voltage between drain and source pins V_{ds} and the drain current I_d coexist during switching from ON to OFF and vice versa, there is an average

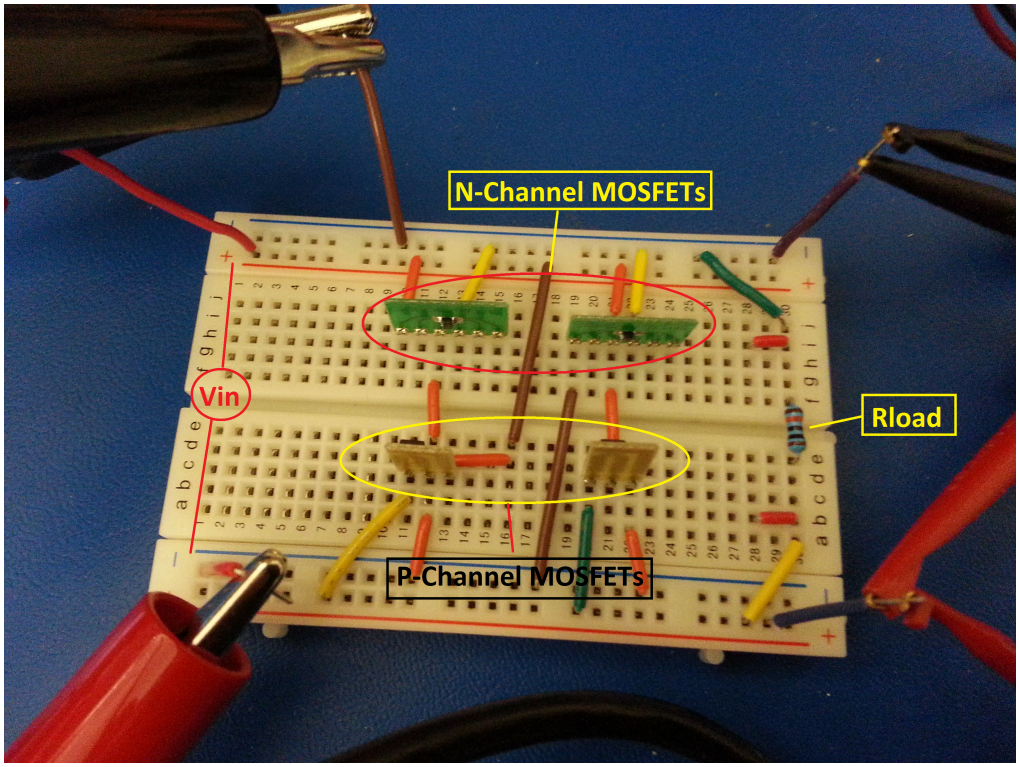

Figure 3.7: Full-wave passive MOSFET rectifier circuit on the breadboard

switching power loss represented by:

$$P_s = \frac{1}{2} V_{ds} I_d f_{sw} (t_{on} + t_{off}) \tag{3.2}$$

where f_{sw} is the switching frequency, t_{on} the on-state time, and t_{off} the off-state time of the MOSFET. To reduce power dissipation in the MOSFET during conduction, we need a small on resistance $R_{DS(on)}$.

3.4 Active Full-Wave MOSFET Rectifiers

Active or synchronous rectifiers can also be found in the literature which increase conversion efficiency by decreasing voltage drop in circuit elements and power losses in switches [28]. Active rectifiers aim to minimize forward voltage drop across the switches, and make switches act like, ideal switch, with zero resistance against current flow. However, they do need control circuitry to synchronize the switch

components, which means additional power consumption in the rectifier circuitry. Since a high efficiency micro-power generator system limits power consumption to the range of nano to micro-watts [27], this places significant constraints on the control circuitry.

A full-wave active MOSFET rectifier schematic is shown in Figure 3.8, which has one extra comparator (LM393-Dual comparator) and one IC MOSFET driver (TC428 Microchip MOSFET driver) with two output pins, compared to the passive MOSFET rectifier.

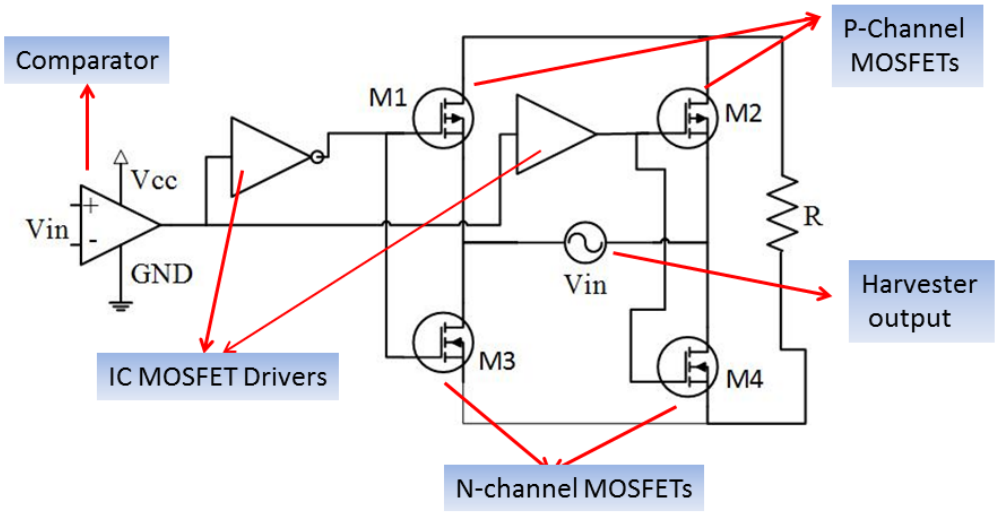

Figure 3.8: Full-wave active MOSFET rectifier circuit

The working principle of a typical active rectifier is as follows: a control circuit drives an FET switch, usually a comparator, defining the ON and OFF states of the switch depending on a voltage comparison of the inverting and non-inverting input pins of the comparator. Sometimes a comparator is not enough to drive the switches, so MOSFET drivers can also be needed, as in our case.

Integrated circuit active rectifiers are a promising possibility because of their low-level power consumption. Their power conversion efficiency is reportedly greater than 80%. Even at low output power levels, 20-30 μW, their efficiency is in the range of 80-90% [26].

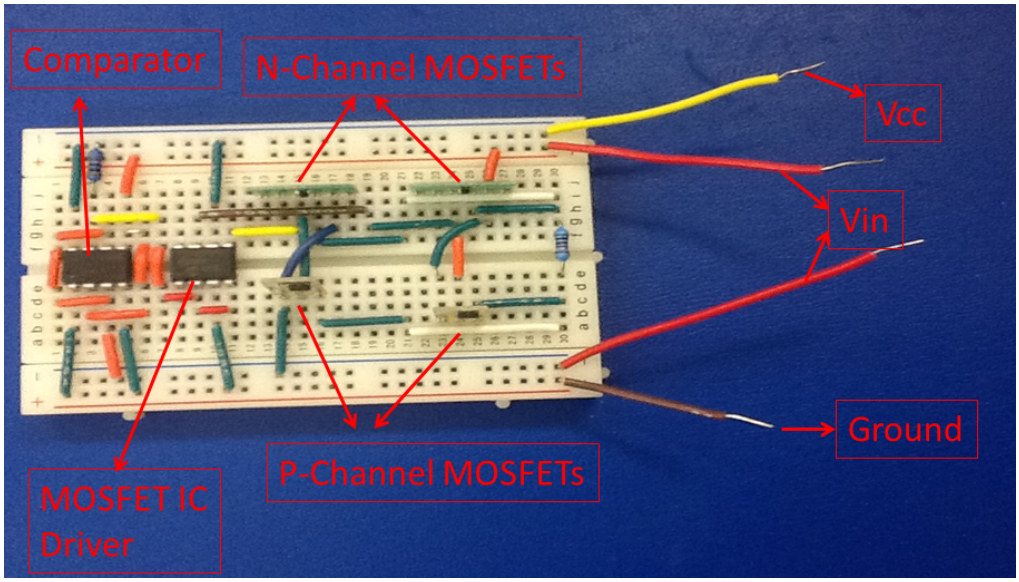

Figure 3.9: Full-wave active MOSFET rectifier circuit on the breadboard

3.5 Baseline Testing of the Passive Full-Wave MOSFET Rectifer

As mentioned in the previous section there are many different full-wave rectifier types, and each uses different electronic devices such as silicon diodes, Schottky diodes, or MOSFETs. Based on the electronic components used they are categorized as: full-wave bridge silicon diode rectifiers, full-wave bridge Schottky diode rectifiers, full-wave passive MOSFET rectifiers, and full-wave active MOSFET rectifiers. In this section we will do simulation of these rectifier types and compare the results. The simulations will be done with LTspice IV software.

Using the simulation results, we calculated the voltage and power efficiency of each rectifier type. Following Peters [27], we define the voltage efficiency η_V as:

$$\eta_V = \frac{V_{out}}{V_{in}} * 100\% \tag{3.3}$$

where V_{out} is the amplitude of the output signal and V_{in} is the amplitude of the

input signal. We also define power efficiency η_P as:

$$\eta_P = \frac{\frac{1}{T}\int_t^{(t+T)} v_{out} i_{out}}{\frac{1}{T}\int_t^{(t+T)} v_{in} i_{in}} * 100\% \tag{3.4}$$

3.5.1 Simulations of Different Full-wave Bridge Rectifier Types in LTspice IV

For the simulation task, we used freeware package LTspice IV, which implements a SPICE simulator of electronic circuits. LTspice IV provided both a schematic capture and waveform for each circuit. Circuit simulations based on transient, AC, noise, and DC and Fourier analysis, can be realized and plotted. The heat dissipation of the components, and efficiency calculation reports, can be obtained from the simulation software, which is produced by semiconductor manufacturer Linear Technology (LTC).

During all simulation tests, a frequency of $f = 100Hz$ and a load R_L=1 kΩ were used. The input signal amplitude values V_{in} ranged from 300 mV to 2V. The amplitude was increased by 100 mV for each step, and for each step we calculated voltage conversion efficiency and power efficiency using Equations 3.3 and 3.4.

3.5.1.1 Full-Wave Silicon Diode Bridge Rectifier

The diode bridge rectifier has been the most-used type for many years, and is well-known. It consists of four silicon diodes in a bridge configuration. The circuit schematic is shown in Figure 3.10.

For 1V input amplitude, the V_{in} and V_{out} signals are shown in Figure 3.10, with the forward voltage drop around 670 mV. In Table 3.1, we list the simulated test data, including V_{in}, V_{out}, voltage conversion efficiency η_V, and power conversion efficiency η_P.

At the minimum applied input amplitude of V_{in}=300 mV, the output voltage amplitude is 7.45 mV, voltage efficiency is 2.48%, and power efficiency is 1.73%. With increasing V_{in}, the voltage and power efficiency also increase. At our max-

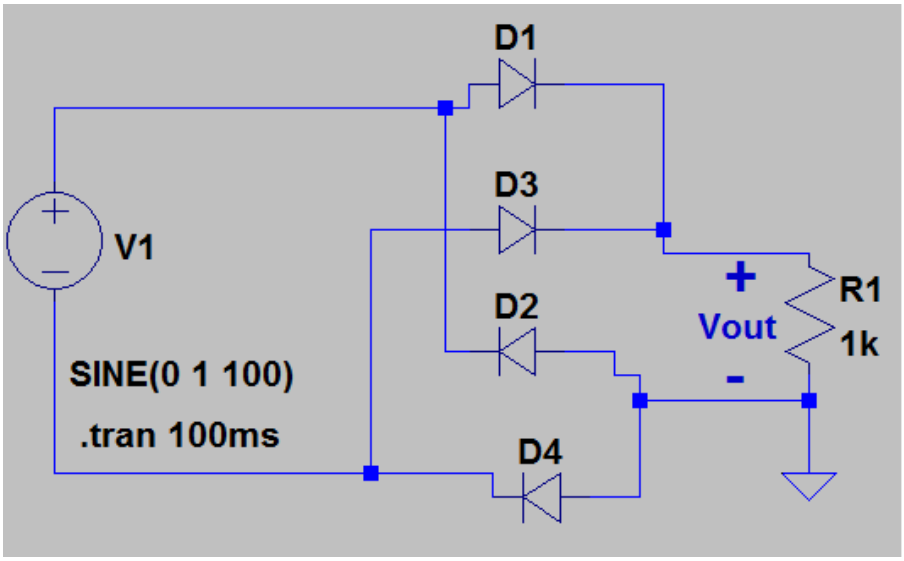

Figure 3.10: Full-wave silicon diode bridge rectifier

imum applied voltage, V_{in}=2V, the voltage efficiency is around 60%, and power efficiency around 55%.

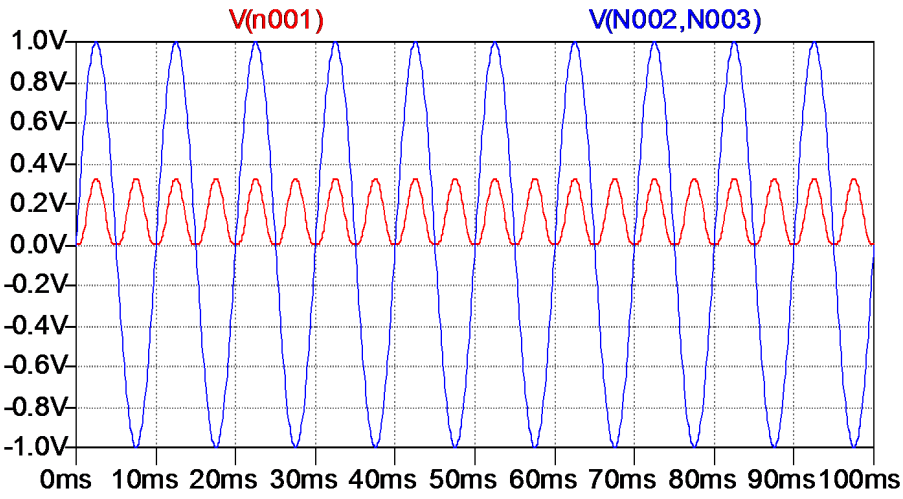

Figure 3.11: V_{in} and V_{out} signals of full-wave silicon diode bridge rectifier, V_{in}=1V, R_L=1 kΩ, f=100Hz

3.5.1.2 Full-wave Schottky Diode Bridge Rectifier

The full-wave Schottky diode bridge rectifier is another type, which uses Schottky diodes, which have a lower forward voltage drop compared to silicon diodes. The circuit schematic is shown in Figure 3.12.

Table 3.1: Full-wave silicon diode bridge rectifier input and output voltage amplitudes, as well as voltage and power efficiency, for R_L=1 kΩ, f=100Hz.

V_{in}(mV)	V_{out}(mV)	Voltage efficiency (η_V) (%)	power efficiency (η_P) (%)
300	7.45	2.48	1.73
400	18	4.5	3.56
500	40	8	6.43
600	76	12.6	10.3
700	126	18	14.77
800	186	23.25	19.39
900	254	28.22	19.39
1000	327	32.7	28.07
1100	405	36.8	31.92
1200	486	40.5	35.44
1300	570	43.84	38.65
1400	655	46.78	41.56
1500	742	49.46	44.22
1600	830	51.87	46.624
1700	920	54.11	48.87
1800	1000	55.55	50.92
1900	1100	57.89	52.80
2000	1190	59.5	54.54

For a 1V input amplitude, the V_{in} and V_{out} signals are shown in Figure 3.13. The forward voltage drop is 300 mV, which is almost 50% less than the silicon diode's. In Table 3.2, we list the simulated test data as V_{in}, V_{out}, voltage conversion efficiency η_V, and power conversion efficiency η_P.

At the minimum applied input amplitude of V_{in}=300 mV, the output voltage amplitude is 90 mV -much higher than silicon diode rectifier- voltage efficiency is 30%, and power efficiency is around 26%. With the increase of V_{in}, the voltage and power efficiency also increase. At our maximum applied input voltage of V_{in}=2V the voltage efficiency is around 83% and the power efficiency around 80%.

3.5.1.3 Full-Wave Passive MOSFET Bridge Rectifier

The full-wave passive MOSFET bridge rectifier is a third type of rectifier which uses two N-channel and two P-channel MOSFETs, connected in a bridge configuration. The circuit schematic is shown in Figure 3.14.

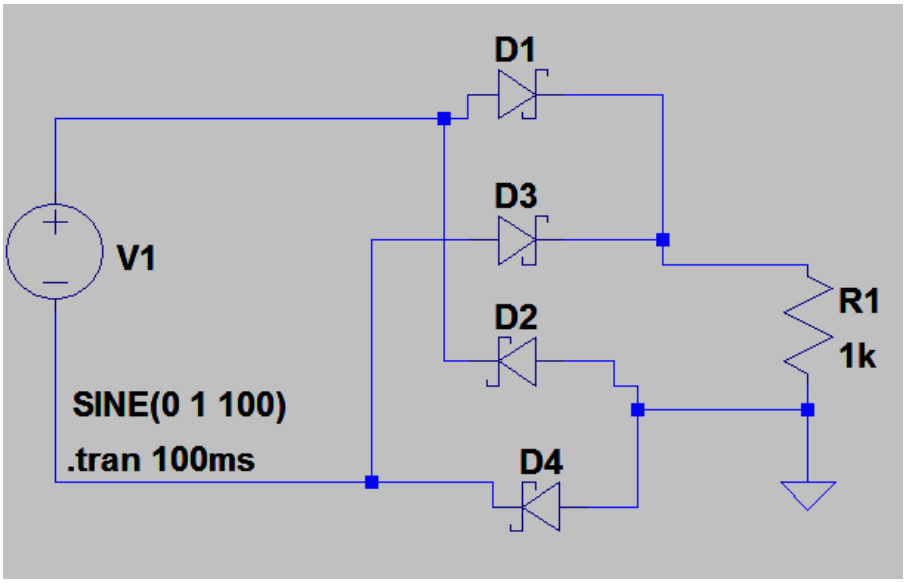

Figure 3.12: Full-wave Schottky diode bridge rectifier

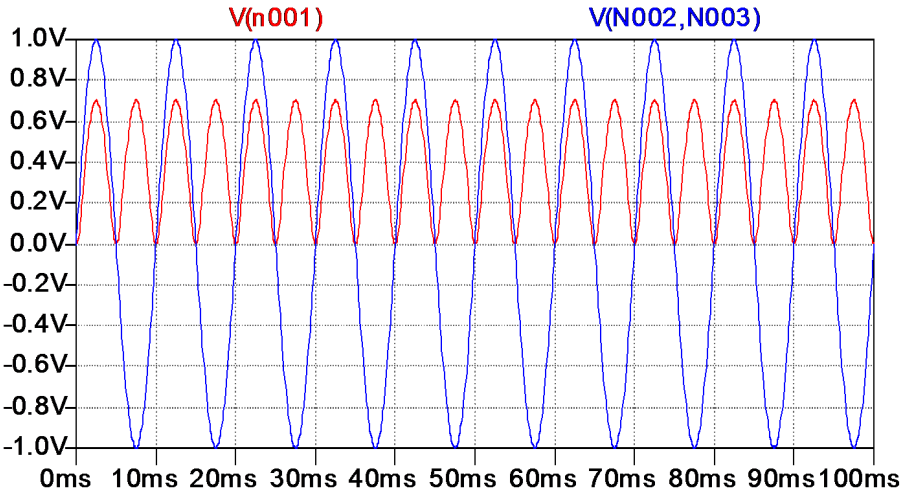

Figure 3.13: V_{in} and V_{out} signals of full-wave Schottky diode bridge rectifier, V_{in}=1V, R_L=1 kΩ, f=100Hz

For an 800 mV input amplitude, the V_{in} and V_{out} signals are shown in Figure 3.15. The voltage drop across the MOSFETs is negligible, which indicates high voltage efficiency. In Table 3.3, we list the simulated test data as V_{in}, V_{out}, voltage conversion efficiency η_V, and power conversion efficiency η_P.

At the minimum applied input amplitude of V_{in}=300 mV, the output voltage amplitude is less than 1 mV-basically the MOSFETs are OFF. Above a 700 mV input voltage, the MOSFETs start conducting, and the output voltage is 330 mV

Table 3.2: Full-wave Schottky diode bridge rectifier input and output voltage amplitudes, as well as voltage and power efficiency, for R_L=1 kΩ, f=100Hz.

V_{in}(mV)	V_{out}(mV)	Voltage efficiency (η_V) (%)	power efficiency (η_P) (%)
300	90	30	25.5
400	164	41	35.9
500	247	49.4	36
600	333	55.5	50
700	423	60.42	55.4
800	514	64.25	59.46
900	607	67.44	62.8
1000	700	70	65.63
1100	794	72.18	68.3
1200	890	74.16	70.10
1300	980	75.38	71.91
1400	1080	77.14	73.48
1500	1170	78	74.9
1600	1270	79.37	76.16
1700	1370	80.58	77.3
1800	1470	81.66	78.31
1900	1560	82.10	79.24
2000	1660	83	80.09

efficiency is 47%, and power efficiency is around 43%. As V_{in} increases, the voltage and power efficiency also increase. At an input voltage of V_{in}=800 mV, the voltage efficiency is around 99%, while power efficiency is over 90%. Maximum power efficiency is over 99% which is a great deal better than of diode-type rectifiers.

3.5.1.4 Full-Wave Active MOSFET Bridge Rectifier

The full-wave active MOSFET bridge rectifier is fourth and last type of rectifier to be studied, which consists of two N-channel and two P-channel MOSFETs. In addition to MOSFETs, it also has two LTC2052 operational amplifiers, and one external DC power supply to energize the amplifiers. The amplifiers are used for applying voltage to the gates of MOSFETs, to switching them ON and OFF. The circuit schematic is shown in Figure 3.16.

For an 800 mV input amplitude, the V_{in} and V_{out} signals are shown in Figure 3.17, and the voltage drop across the MOSFETs is negligible, which means

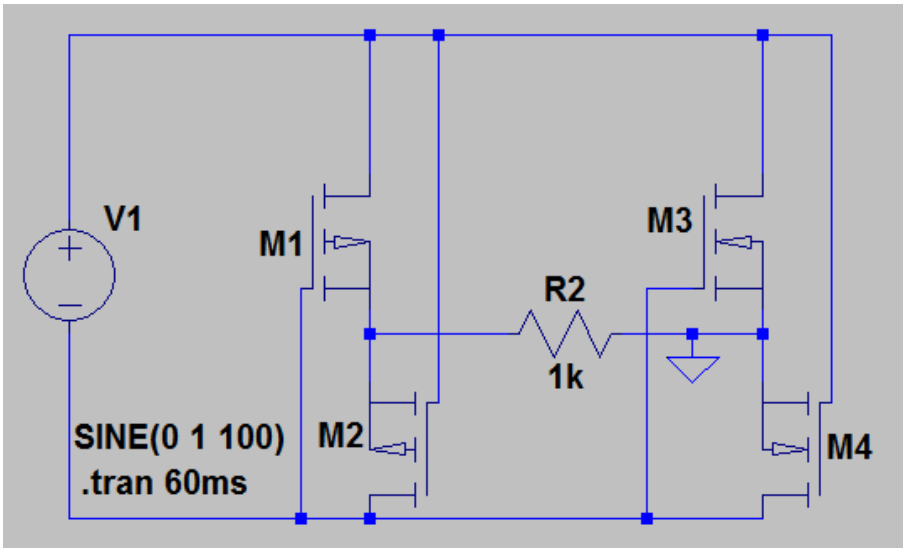

Figure 3.14: Full-wave passive MOSFET bridge rectifier

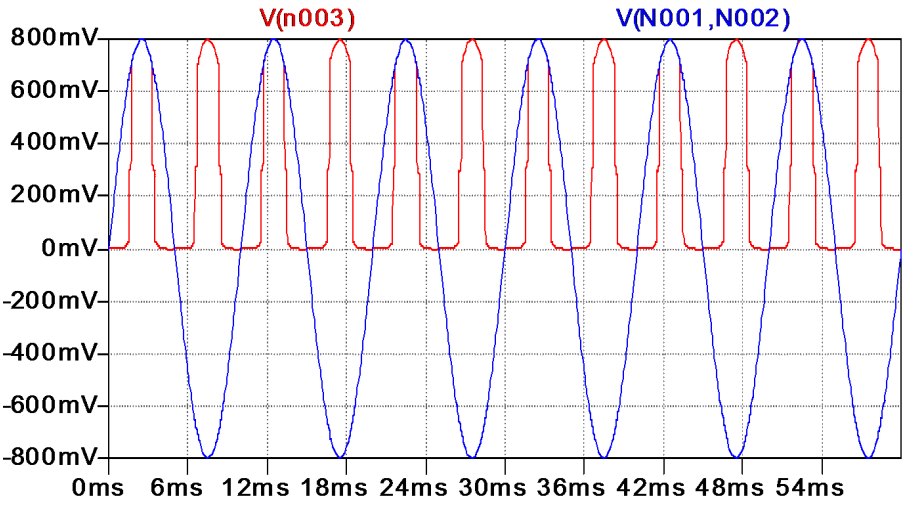

Figure 3.15: V_{in} and V_{out} signals of full-wave passive MOSFET rectifier, V_{in}=800 mV, R_L=1 kΩ, f=100Hz

high voltage efficiency. In Table 3.4, we present the simulated test results, with V_{in}, V_{out}, voltage conversion efficiency η_V, and power efficiency η_P.

At the minimum applied input amplitude of V_{in}=300 mV the output voltage amplitude is around 15 mV, and basically the MOSFETs can be treated as an open switch. Above a 500 mV input voltage, the MOSFETs start conducting with a 149 mV output voltage; voltage efficiency is around 30%, and power efficiency around 17%. As V_{in} increases, the voltage conversion efficiency and power efficiency also

Table 3.3: Full-wave passive MOSFET bridge rectifier input and output voltage amplitudes, with voltage and power efficiency, for R_L=1 kΩ, f=100Hz.

V_{in}(mV)	V_{out}(mV)	Voltage efficiency (η_V) (%)	power efficiency (η_P) (%)
300	0.056	0.01	0.0013
400	0.4	0.1	0.017
500	2.5	0.5	0.028
600	14	2.33	1.78
700	330	47.14	43.67
800	799	99.8	94.67
900	899	99.9	97.38
1000	999	99.9	98.38
1100	1099	99.9	98.76
1200	1199	99.9	99.13
1300	1299	99.9	99.31
1400	1399	99.9	99.37
1500	1499	99.9	99.52
1600	1599	99.9	99.59
1700	1699	99.9	99.66
1800	1799	99.9	99.76
1900	1899	99.9	99.74
2000	1999	99.9	99.78

increase.

There are current peaks when switching the MOSFETs ON and OFF; the reason is that during ON and OFF switching, there is a short period when the two N-channel MOSFETs are ON at the same time, which creates a short circuit loop. The turn-on delay time $t_{d(on)}$ is much shorter than turn-off delay time $t_{d(off)}$; as a result M4 MOSFET turns ON before M3 MOSFET has turned OFF, and vice versa. The turn-on delay time for N-channel MOSFETs (M3-M4) is typically 19.5 ns, and the turn-off delay time is 173 ns [36].

We have over 90% voltage efficiency starting at an 800 mV input voltage, while for power efficiency we reach 90% at a 1V input voltage. We have maximum voltage efficiency and maximum power efficiency at around 99%.

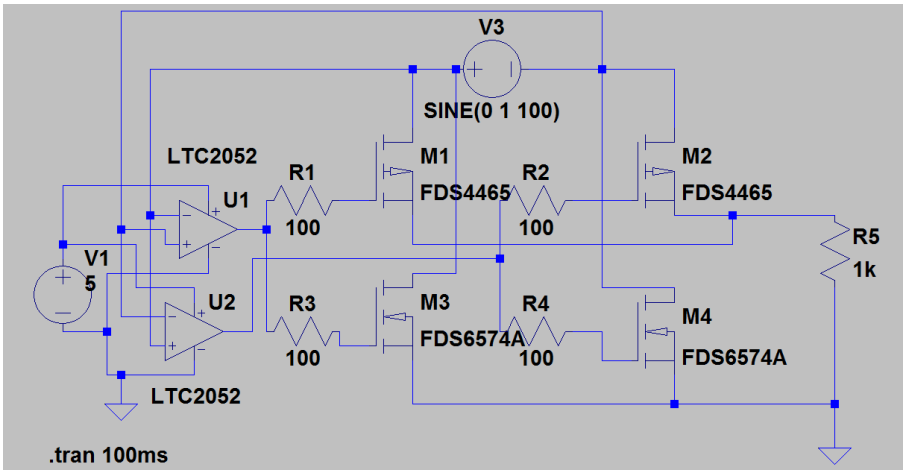

Figure 3.16: Full-wave active MOSFET bridge rectifier

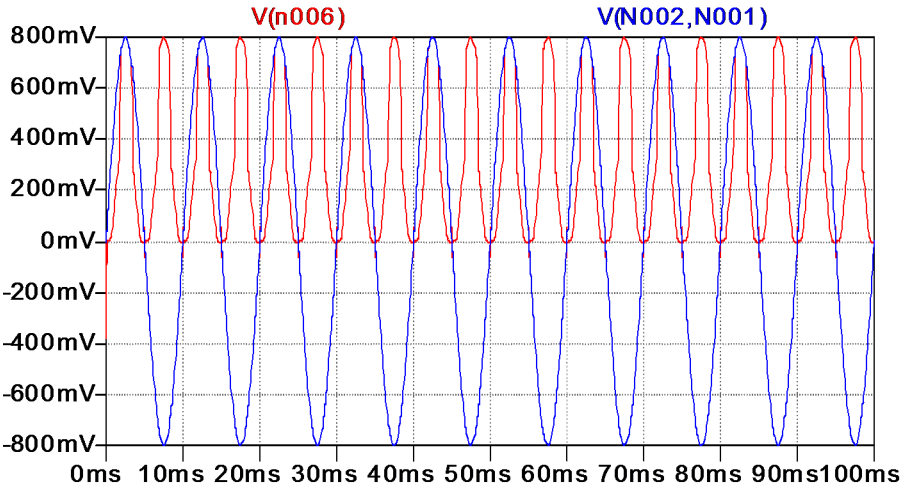

Figure 3.17: V_{in} and V_{out} signals of full-wave active MOSFET rectifier, V_{in}=800 mV, R_L=1 kΩ, f=100Hz

3.6 Comparison of Full-wave Rectifiers Simulation Results

We have simulated our four different types of full-wave bridge rectifier under the same conditions, and tabulated the output voltages V_{out} across the electrical load (R_L=1 kΩ), the voltage efficiency η_V, and the power efficiency η_P for each input voltage amplitude V_{in}.

As can be seen in Figure 3.18, for voltage efficiency the worst type of rectifier is the silicon diode full-wave bridge rectifier, which has a maximum voltage efficiency

Table 3.4: Full-wave active MOSFET bridge rectifier input and output voltage amplitudes, with voltage and power efficiency, for R_L=1 kΩ, f=100 Hz.

V_{in}(mV)	V_{out}(mV)	Voltage efficiency (η_V) (%)	power efficiency (η_P) (%)
300	14	4.66	0.39
400	70	17.5	6.24
500	149	29.8	17.2
600	238	39.6	27.36
700	328	46.85	35.65
800	798	99.75	82
900	898	99.8	88.67
1000	998	99.9	91.84
1100	1099	99.9	93.67
1200	1199	99.9	94.87
1300	1299	99.9	95.68
1400	1399	99.9	96.35
1500	1499	99.9	96.81
1600	1599	99.9	97.19
1700	1699	99.9	97.47
1800	1799	99.9	97.73
1900	1899	99.9	97.95
2000	1999	99.9	98.11

of around 60%. Up to a 600 mV input amplitude, the Schottky diode full-wave rectifier has a higher voltage efficiency than the other three types. In terms of reaching the maximum voltage efficiency, passive and active MOSFET-type rectifiers are the leaders, both of them having 99% voltage efficiency beyond an 800 mV input voltage. It is clear that up to a 700 mV input voltage, the Schottky diode has the best voltage efficiency, while above a 700 mV input voltage, the MOSFET rectifiers have the highest voltage efficiency.

From Figure 3.19 we can say that, in terms of power efficiency, the worst type of rectifier is again the silicon diode bridge, which has a maximum power efficiency around 54%. Up to a 700 mV input amplitude the Schottky diode full-wave rectifier has higher power efficiency than the other three types. In terms of reaching the highest voltage efficiency MOSFET-type rectifiers are the best, with 99% power efficiency above an 800 mV input voltage.

Since there is no significant difference between active and passive MOSFET

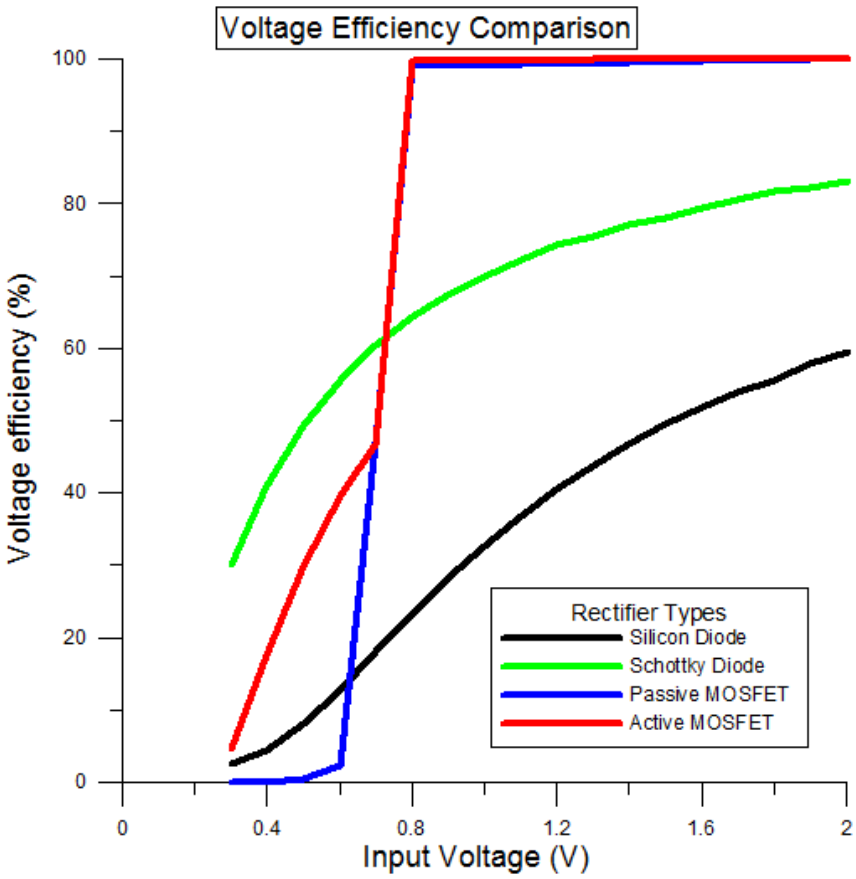

Figure 3.18: Voltage efficiency comparison of rectifiers

rectifiers, we decided to use a passive MOSFET rectifier to test with the harvester. Even though an active MOSFET rectifier has higher power efficiency than a passive one between 300 mV to 600 mV, it is not preferred, because it needs DC power supply, as well as having a start-up issue in that kind of active rectifiers [29]. An active rectifier means having extra active components, greater complexity, and larger PCB size, which is very important in wearable systems.

Considering both voltage and power efficiency the full-wave passive MOSFET rectifier seems the best option to achieve highly efficient rectification in harvesters.

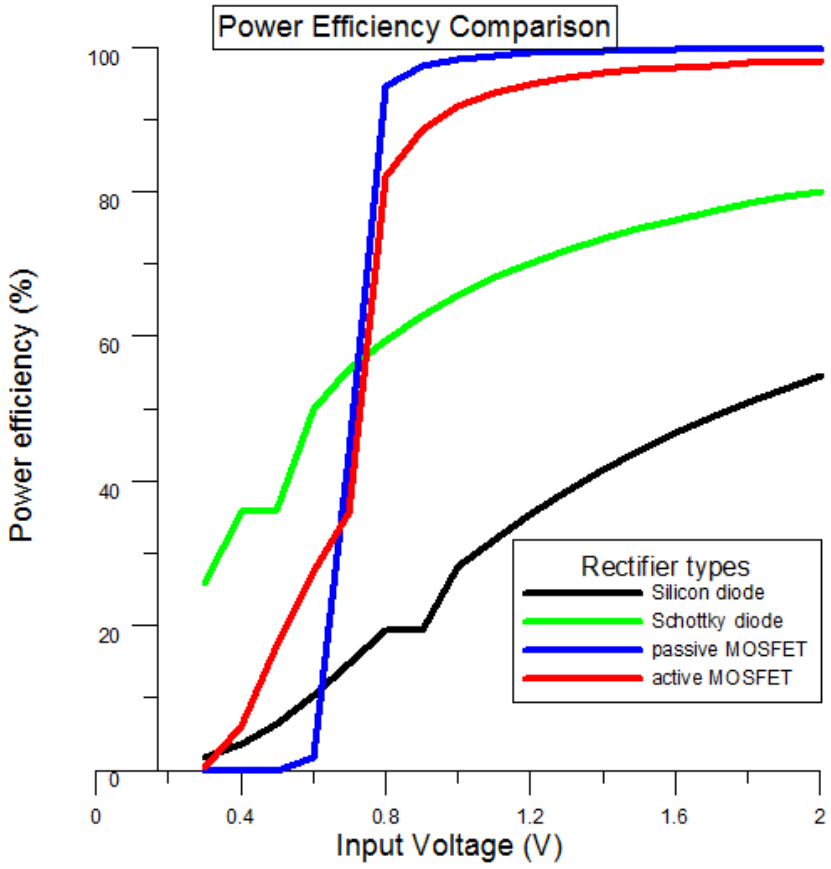

Figure 3.19: Power efficiency comparison of rectifiers

3.7 Testing A Passive Full-Wave MOSFET Rectifier With Function Generator

The passive full-wave MOSFET rectifier has been implemented using Commercial Off-the-Shelf (COTS) components on a breadboard, and the rectifier was tested using a function generator for different AC voltage source amplitudes. The source frequency was always set to 100Hz during the tests, and the load was an R_L=1 kΩ pure resistive load.

As a minimum applied AC voltage amplitude, 300 mV was used, with the amplitude increased to 1.25V in 50 mV steps. We observed that up to a 550 mV input amplitude, the output RMS voltage is less than 100 mV, with a voltage efficiency of less than 30%. Above a 700 mV input voltage amplitude, we found

output RMS voltage, around 280 mV, with over 50% voltage efficiency.

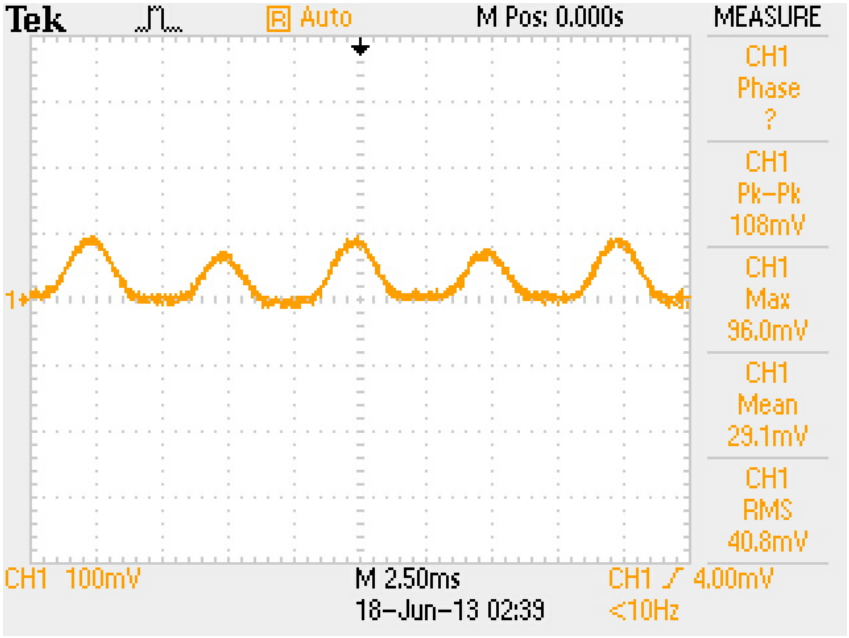

Figure 3.20: Rectified signal for the 300 mV input amplitude

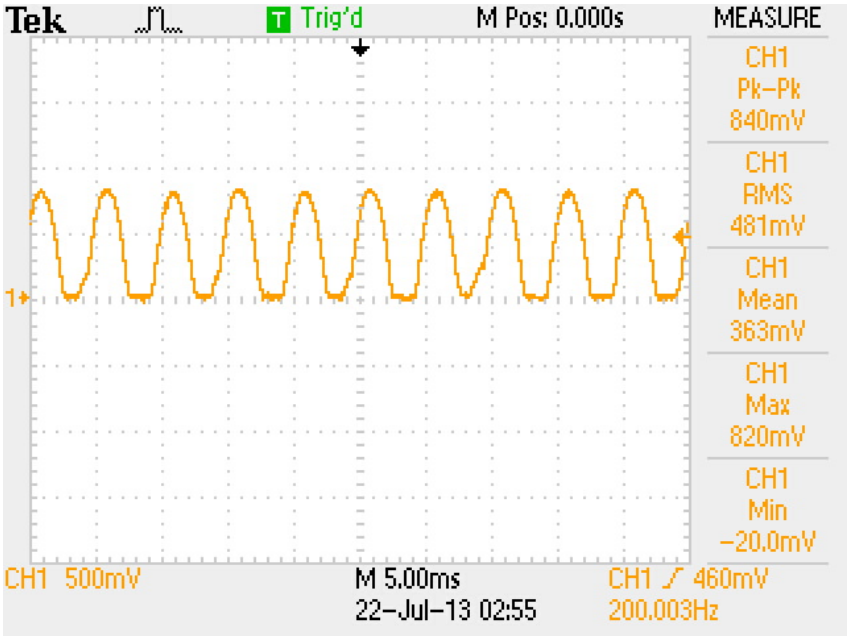

Figure 3.21: Rectified signal for the 850 mV input amplitude

In Table 3.5, we tabulate the input voltage, RMS output voltage, and voltage

efficiency:

$$\eta_V = \frac{V_{out(rms)}}{V_{in(rms)}} \tag{3.5}$$

Table 3.5: Full-wave passive MOSFET rectifier input and output voltage values and voltage efficiency, using a function generator

V_{in}(mV)	$V_{out(rms)}$(mV)	Voltage efficiency (η_V)(%)
300	22	10
350	26	10
400	28.5	10
450	40	12
500	65	18
550	107	27
600	162	37
650	224	48
700	288	57
750	352	66
800	416	73
850	481	79
900	527	82
950	575	85
1000	618	87
1050	660	88
1100	701	89
1150	740	90
1200	778	91
1250	815	91.8

Table 3.5 shows the applied input AC voltage V_{in} and the rectified RMS output voltage V_{out} across the resistive load R_L=1 kΩ, with voltage efficiency calculated by Equation 3.5. The voltage efficiency starts from 10% for the minimum applied input, and increases to 92% for a 1.25V applied input voltage.

When we applied a 300 mV amplitude input signal, we were able to see a 100 mV rectified signal across the load; this is our minimum input voltage where we can use our rectifier to rectify the AC signal, as seen in Figure 3.20. Figure 3.21 also shows the rectified output signal across the load.

For the highest applied input voltage of 1.25V, we are able to see an 815 mV

RMS output rectified signal across the load.

In Table 3.6, calculated power efficiency of passive MOSFET is presented, along with the applied voltage as tested with a function generator. For calculations, we measured the input current I_{in}, and since we know V_{in}, then we were able to calculate input power by Equation 3.6. We also calculated the output power by Equation 3.7, so as to calculate power efficiency by Equation 3.8. Above a 700 mV applied voltage, we get over 90% power efficiency in the rectifier.

$$P_{in} = V_{in} I_{in} \tag{3.6}$$

$$P_{out} = \frac{(V_{out})^2}{R_L} \tag{3.7}$$

$$\eta_P = \frac{P_{out}}{P_{in}} \tag{3.8}$$

Table 3.6: Full-wave passive MOSFET rectifier input voltage values and power efficiency using a function generator

V_{in}(mV)	Power efficiency (η_P)(%)
500	52
600	84
700	92
800	95
900	97.9
1000	98
1100	99.3
1200	99.9
1300	99.9
1400	99.9
1500	99.9

3.8 Testing of Active Full-Wave MOSFET Rectifier With Function Generator

We have implemented the active full-wave MOSFET rectifier using commercial off-the-shelf components on a breadboard, and we tested it with a function generator for different AC voltage amplitudes. The source frequency was always set to 100Hz during the test, and load was R_L=1 kΩ and purely resistive. We started by applying an AC signal amplitude of 200 mV to the rectifier, and increased the amplitude step by step up to 1.25V.

Figure 3.22 shows output voltage across the load R_L for a 500 mV input amplitude. As can be seen,we have some voltage peaks between period ends and beginnings, which is caused by MOSFET switching synchronization problem. To cancel out these peaks, we should use delay circuits after drivers to achieve synchronization in switching periods, so that we can prevent both MOSFETs being ON at the same time.

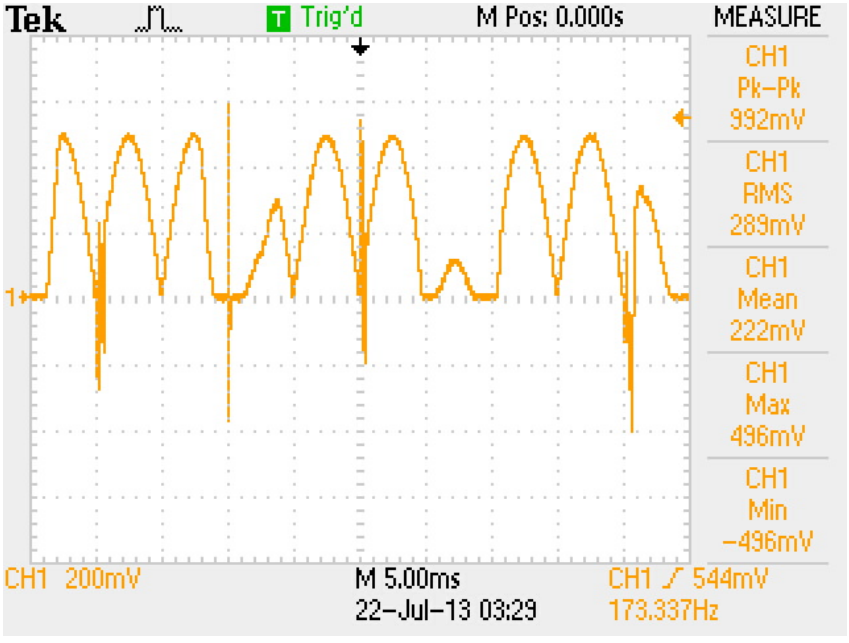

Figure 3.22: Rectified signal for the 500 mV input amplitude

In Table 3.7, the voltage and power efficiencies are calculated in RMS unit base, so all measurements and calculations are made based on RMS values. The voltage

and power efficiency calculation equations are the same as in the previous section. Even though we found high voltage efficiency at small input values, this was not the case for power efficiency.

Table 3.7: Full-wave active MOSFET rectifier input and output voltage values, as well as voltage and power efficiency, as tested with a function generator

V_{in}(mV)	$V_{out(rms)}$(mV)	Voltage efficiency(rms)(%)	Power efficiency(rms)(%)
200	87	61	4.5
250	120	67	6.7
300	150	70	8
350	186	74	9.6
400	220	77	17
450	247	77	23
500	280	78	27
550	321	82	32
600	353	82.8	36
650	390	84.5	45
700	430	89	57
750	474	90	60
800	512	90	61
850	538	91	62
900	584	91	68
950	614	91	68
1000	660	92	75
1050	698	93	75
1100	737	94.3	81
1150	774	94.7	85
1200	808	94.8	45
1250	843	94.9	89

Chapter 4

Passive MOSFET Rectification in Electromagnetic Harvesters

4.1 Maximum Power Extraction in Electromagnetic Harvester

In order to obtain maximum power from an electromagnetic harvester the excitation source frequency should be equal to the harvester's natural frequency, thus there is a need to know the natural frequency f_n of the harvester [24]. To determine f_n, the harvester was mounted on the shaker platform firmly, and then the excitation frequency of the shaker was swept up and down in the neighbourhood of the natural frequency value.

Natural Frequency was studied for three different cases, to see the possible effects of each case. In the first case, the harvester's output terminals were left open (open-circuit), which symbolized the infinite load at the end. As a second case, a rectifier was connected to the harvester, and output was again left open, to see the effect of the rectifier on the harvester. For the third case, we tried to see what would happen if we connected a resistive load to our system, so we connected a 1 kΩ resistor as a load.

We used the same test setup for all three case; the settings were as follows:

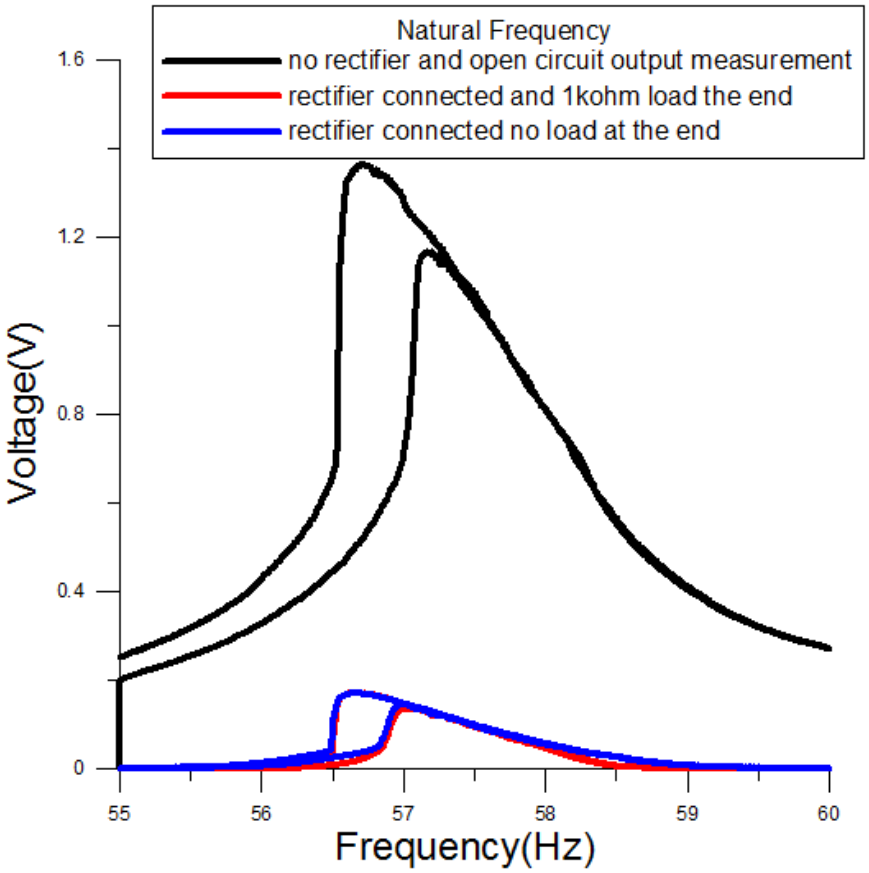

Figure 4.1: Frequency-response curves for the electromagnetic harvester: a) harvester alone, b) rectifier connected to harvester and R_L=1 kΩ load, c) rectifier connected but no load.

starting frequency is 55Hz, it then sweeps up to 60Hz, then down from 60 to 50Hz; base acceleration amplitude was 0.5g, the sweep rate was 1 Hz/min, and each test duration was 10 minutes, so we could see up-sweep and down-sweep effects together.

The test results for all cases are shown in Figure 4.1; as can be seen from the graph, in the first case, the peak frequency was 57.15Hz for up-sweep and 56.7Hz in the down-sweep. The maximum output voltage values were 1.167V and 1.362V for the up-sweep and down-sweep cases respectively.

On the other hand, in the second case the natural frequency was 56.99Hz for up-sweep and 56.67Hz for down-sweep, while the maximum output voltages were 146 mV and 170 mV for up-sweep and down-sweep respectively.

In the last case, the natural frequency is the same as in the second case, which

indicates that a 1 kΩ load acts like an open circuit to the harvester, which means the harvester's optimum load is less than 1 kΩ.

As seen from the frequency-response curve, the peak frequency does not change much with a rectifier circuit, which indicates that the rectifier circuit acts like a resistive load.

4.1.1 Optimum Load Measurements of the Harvester With and Without Rectifier Circuitry

Maximum power transfer from the harvester to the electrical load, can be achieved when the input impedance of the interface circuit is the complex conjugate of the energy harvester's output impedance.

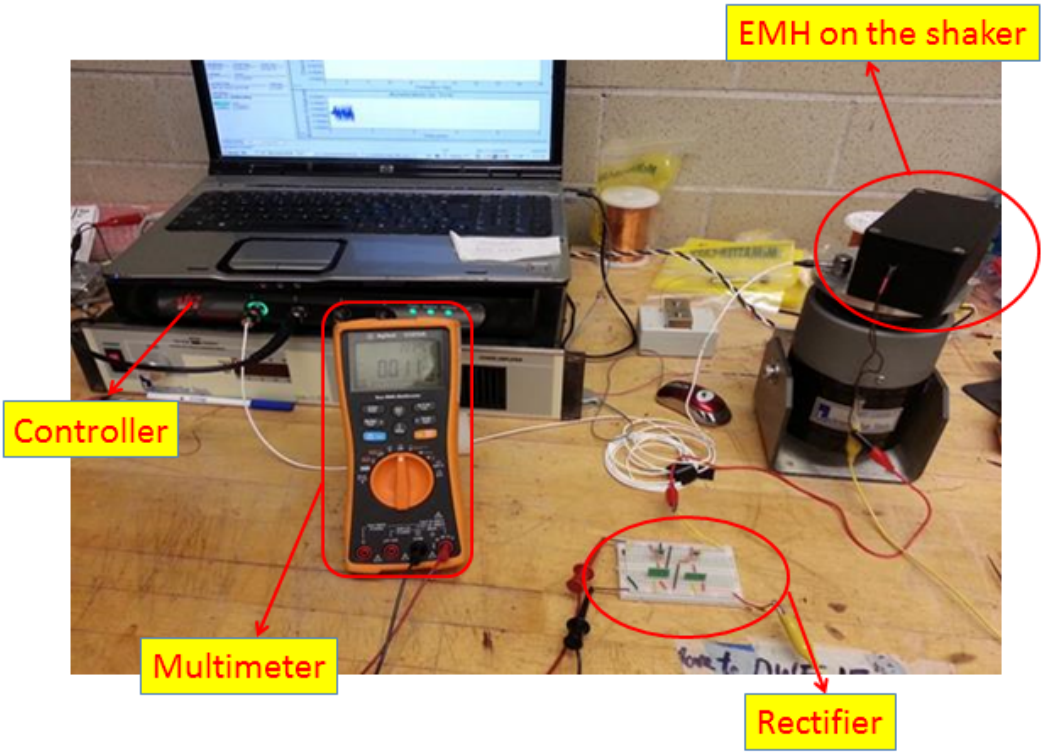

Figure 4.2: Optimum load test setup with rectifier circuit

In order to define the optimum power transfer condition for our electromagnetic harvester, we tested the harvester under two cases. In the first case, with the

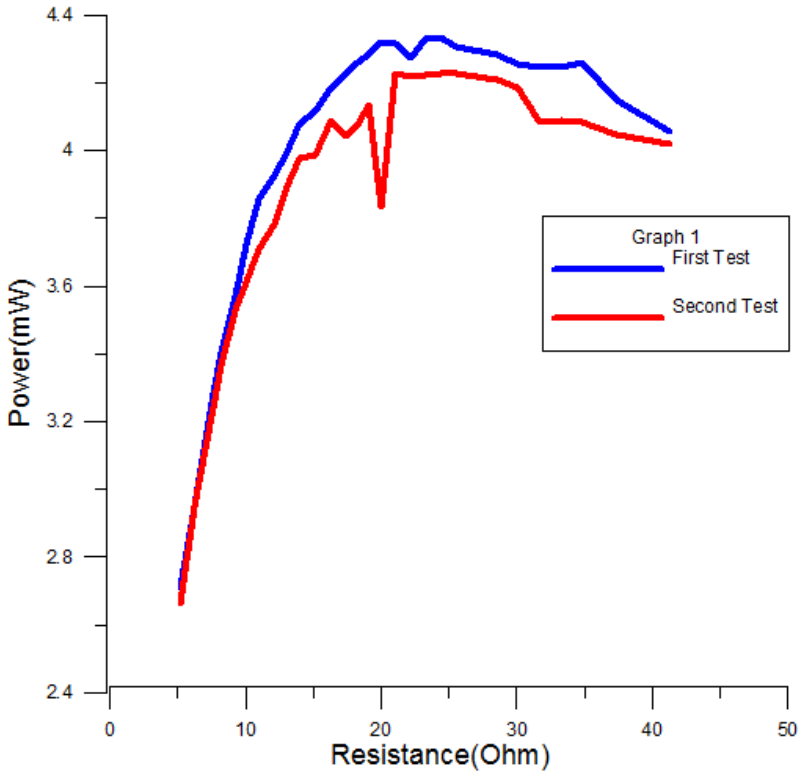

Figure 4.3: Optimum load graph without rectifier circuit

harvester's output terminals only connected to a resistive load without a rectifier, and in the second case with both rectifier and load were connected to the harvester. The test setup can be seen in Figure 4.2 for the second case.

During each test, we excited the shaker to the harvester's natural frequency 56.90Hz,and used a 0.5g acceleration amplitude for 1 minute. RMS output voltage value was measured with a true RMS multimeter, so as to calculate output power from Equation 3.7.

For the first case, the load resistance R_L was varied using small intervals from 5.14 Ω to 41.2 Ω, so as to find optimum load precisely. For this case, the obtained power varied from 2.6 mW to 4.3 mW, and the maximum power was received when the resistance is 24 Ω, as can be seen in Figure 4.3.

For the second case, we also changed the resistance value by 10 Ω intervals from 10 Ω to 100 Ω, and the power varied from 0.71 mW to 1.52 mW. The maximum power was achieved when 46 Ω was connected to the rectifier, as can be seen in

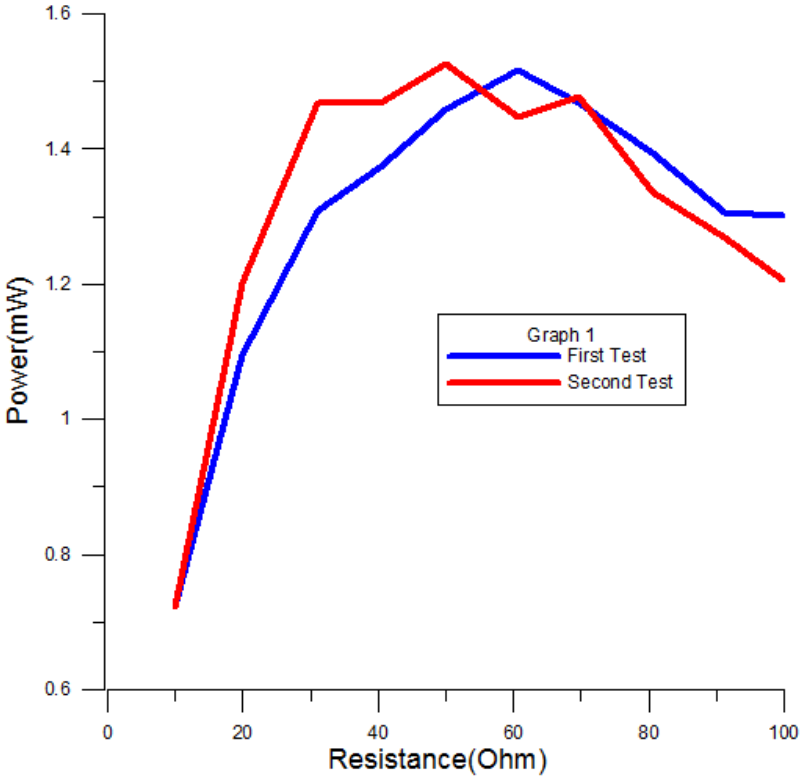

Figure 4.4: Optimum load graph with rectifier circuit

Figure 4.4.

4.1.2 Impedance Measurements for the Passive MOSFET Rectifier

In order to achieve maximum power transfer from the mechanical domain to the electrical domain, the harvester's output impedance amplitude should be equal to the rectifier's input impedance amplitude.

The test setup seen in Figure 4.5 was used to calculate the input impedance Z_{in} of the rectifier. In the test setup, we have a Tektronix AFG3022B function generator as an AC source, and an Agilent U1272A hand-held digital multimeter to measure the I_{in}. We set the AC voltage source amplitude to 1V, and changed its frequency each time by a 10Hz interval from 10Hz to 100Hz, to see the impedance change versus frequency. A Tektronix TDS 2004C four channel digital storage

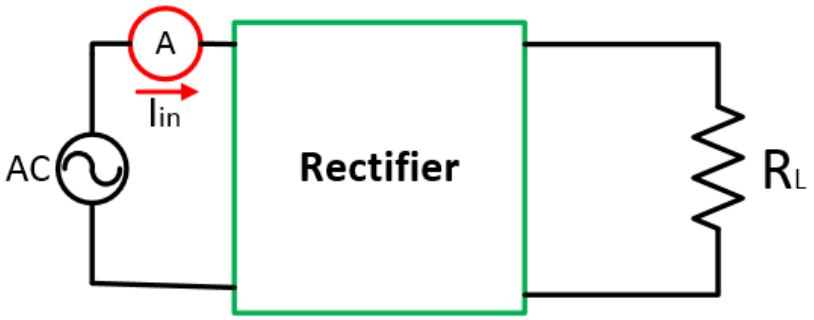

Figure 4.5: Input impedance measurement test schematic

oscilloscope was used to measure the RMS value of the AC voltage source.

In the input impedance measurement, we used two different cases: in the first case there was no load connected to harvester, basically it was an open circuit, while in the second case, there is a resistive load at the end.

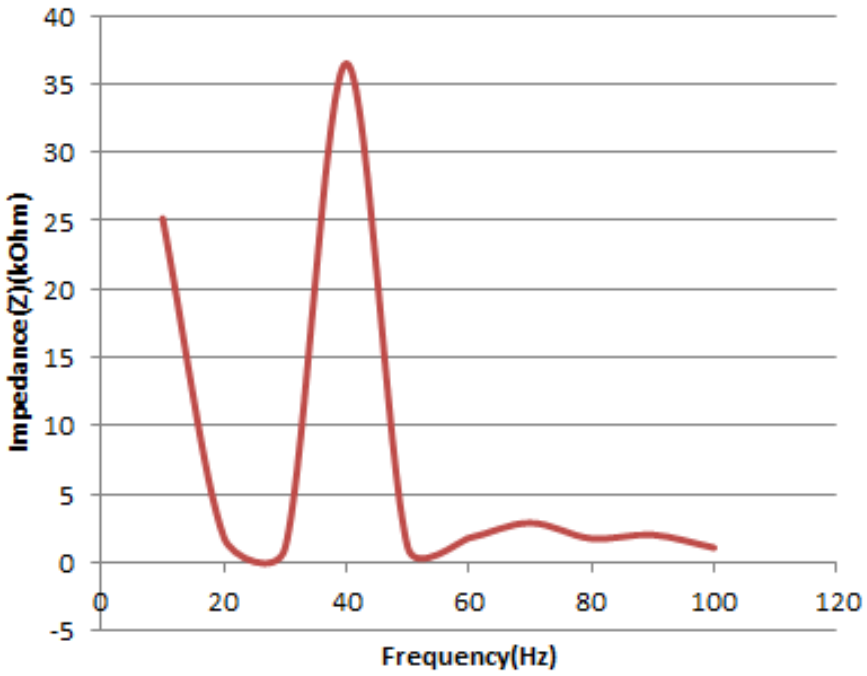

Figure 4.6: Input impedance Z_{in} vs frequency, when the output is an open circuit

Once we have the current and voltage RMS values for the first case, then we employ Ohm's law, Equation 4.1, which defines the relation between current and voltage, to calculate the value of the input impedance Z_{in} shown in Figure 4.5.

For the second case, we had a R_L=101 kΩ resistive load connected to the output terminal of the rectifier. We repeated the same test we had used for the first case, and obtained the results shown in Figure 4.7.

$$Z_{in} = \frac{V_{in}}{I_{in}} \tag{4.1}$$

As seen in Figure 4.6, the input impedance has a peak value of 36 kΩ around 40Hz, and has two zeros, one at 26Hz and the other at 56Hz. For the frequency values higher than 60Hz the input impedance shows stable behaviour, and stays around 2 kΩ.

For the case with load, we found a 14 kΩ peak impedance value at 30Hz, which decreased to 2 kΩ above 60Hz, just as in the previous case.

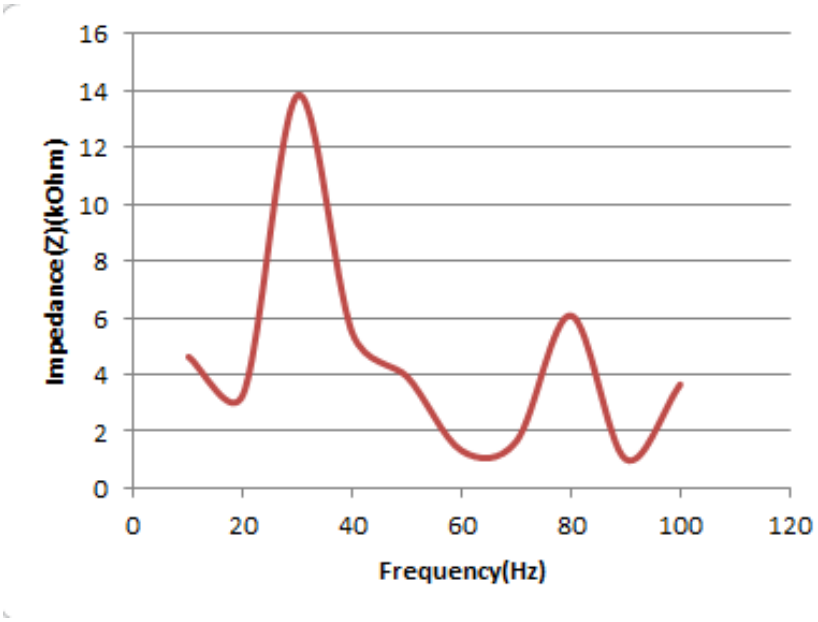

Figure 4.7: Input impedance Z_{in} vs frequency with a resistive load at the output of the rectifier

4.2 Testing the Passive MOSFET Rectifier With Harvester

We tested the full-wave passive MOSFET rectifier with an electromagnetic harvester at its natural frequency (f=56.9Hz) for different base acceleration amplitude (g) values. We calculated voltage efficiency for each input voltage associated with given g when a load of 101 kΩ, as shown in Table 4.1.

Table 4.1: Full-wave passive MOSFET rectifier input/ output voltage amplitudes and voltage efficiency test results as tested with a harvester

V_{in}(mV)	V_{out}(mV)	Voltage conversion efficiency (η_V) (%)
290	44	15
308	48	15
320	72	22.5
400	176	44
502	416	82
600	596	99.9
720	719	99.9
1230	1220	99.9
1310	1300	99.9

For the optimum load of R_L=46.4 Ω at different acceleration g values, the power efficiency of passive MOSFET rectifier was calculated, as shown in Figure 4.8. As we increase the acceleration amplitude, the power efficiency also rises, because the increase in g leads to an increase in the output voltage of the harvester.

4.3 Implementation of the Passive MOSFET Rectifier on the Printed Circuit Board(PCB)

We designed the passive MOSFET rectifier to implement on a PCB using off-the-shelf components; the PCB layout of the rectifier can be seen in Figure 4.9. We have P-channels on the left-hand side, and N-channels on the right-hand side, of the PCB. All components are surface-mount type, and there was no need to drill holes which is the case for through-mount type components. After designing the

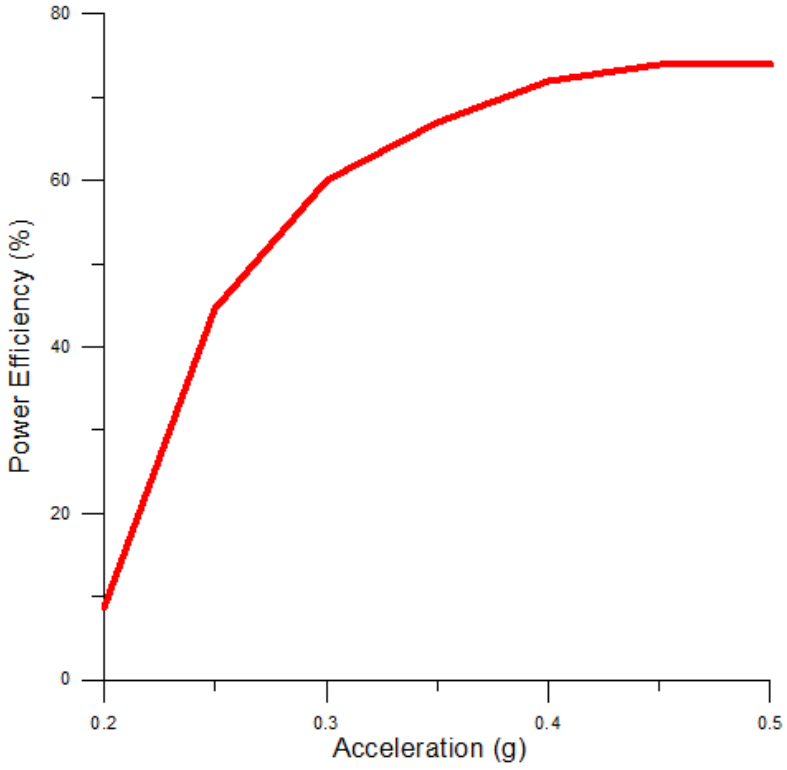

Figure 4.8: Power efficiency vs acceleration amplitude (g) for passive MOSFET rectifier

layout, we sent it to PCB fabricators to produce for us. Our circuit dimension is 2.54 cm x 2.54 cm, roughly the size of a Canadian two-dollar coin. After receiving the PCB, we soldered our MOSFETs on it as shown in Figure 4.11, and tested it with a function generator.

We tested it with the function generator to see its functionality as it rectified the input signal, and because of system noise, the waves were not so clean. We also soldered a 220 μF capacitor, Figure 4.13, as a smoothing capacitor, and with a smoothing capacitor the ripples were cancelled, and we achieved pure DC voltage at the end, as seen in Figure 4.14.

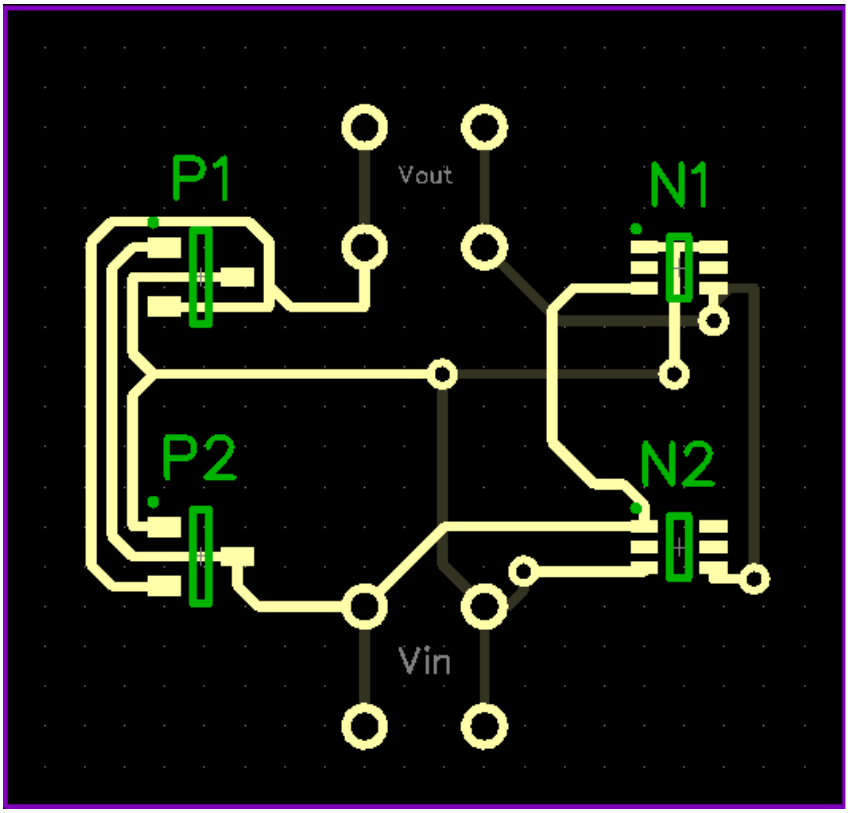

Figure 4.9: PCB layout of passive MOSFET rectifier

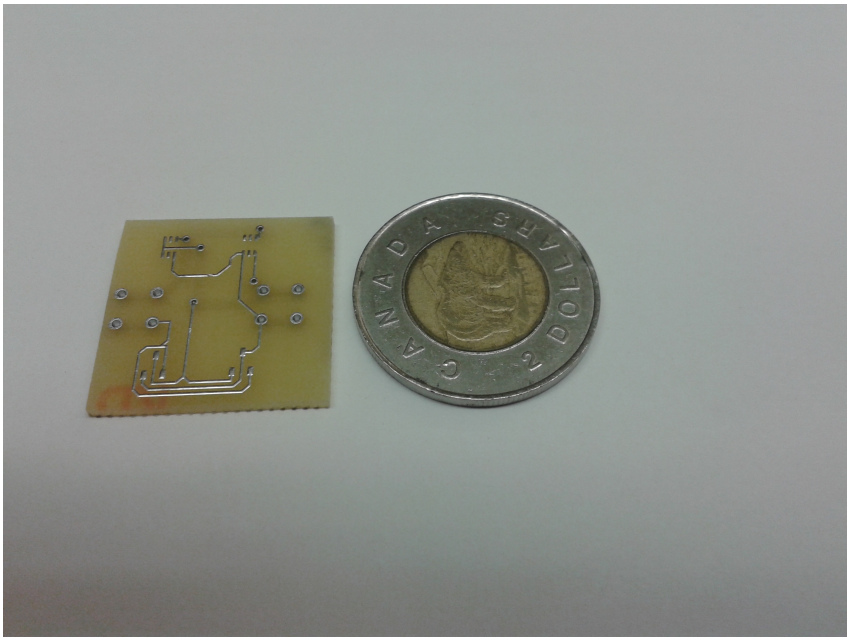

Figure 4.10: Fabricated PCB of passive MOSFET rectifier and toonie

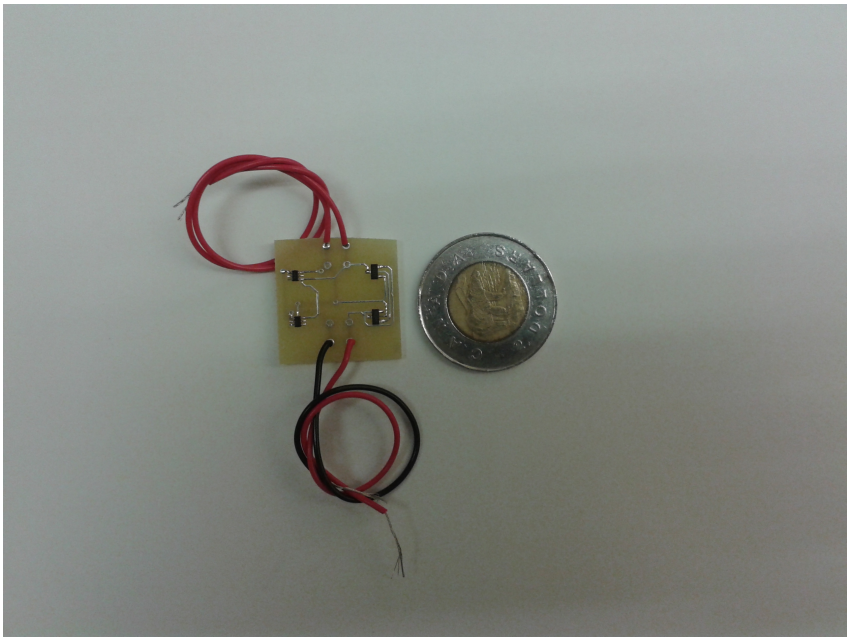

Figure 4.11: PCB assembly of passive MOSFET rectifier

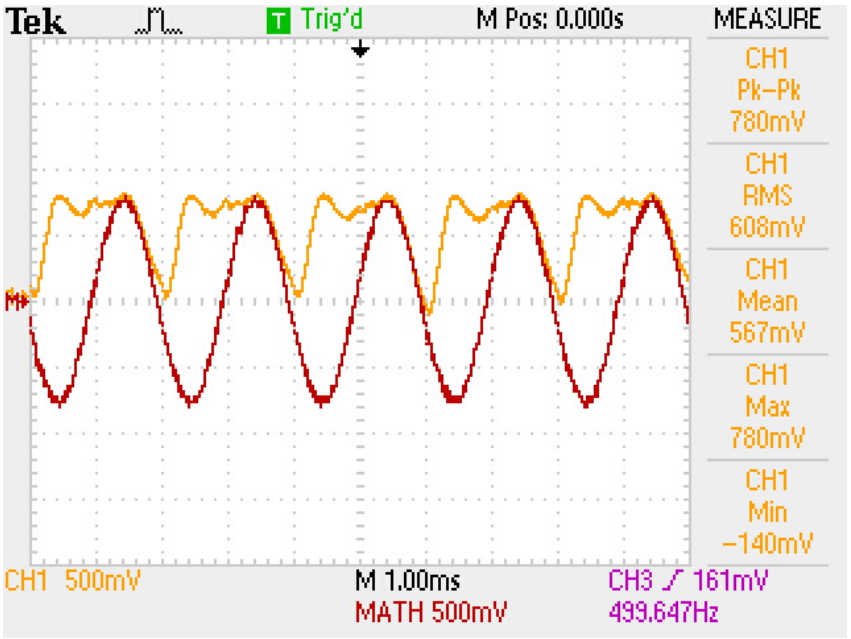

Figure 4.12: Input and output signals of the PCB test

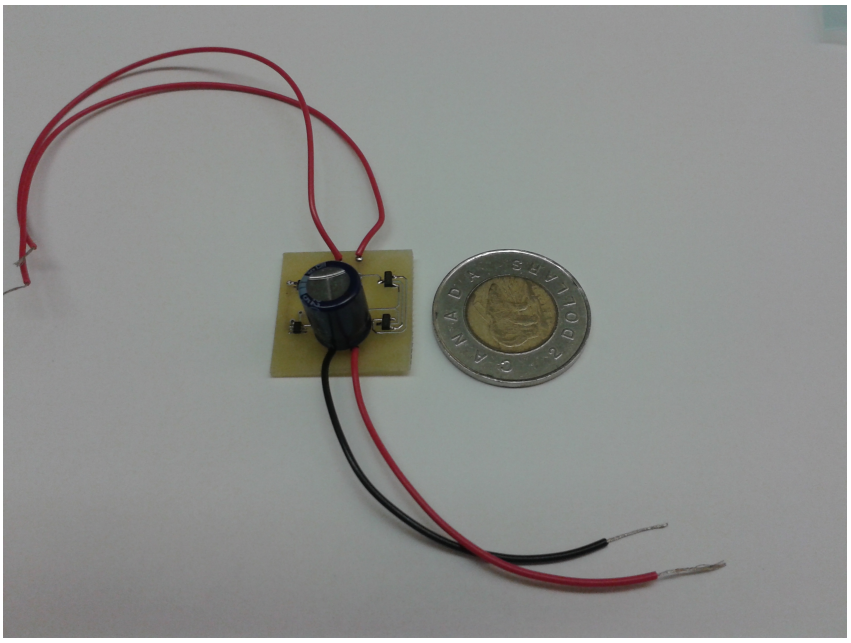

Figure 4.13: Capacitor added to PCB and toonie

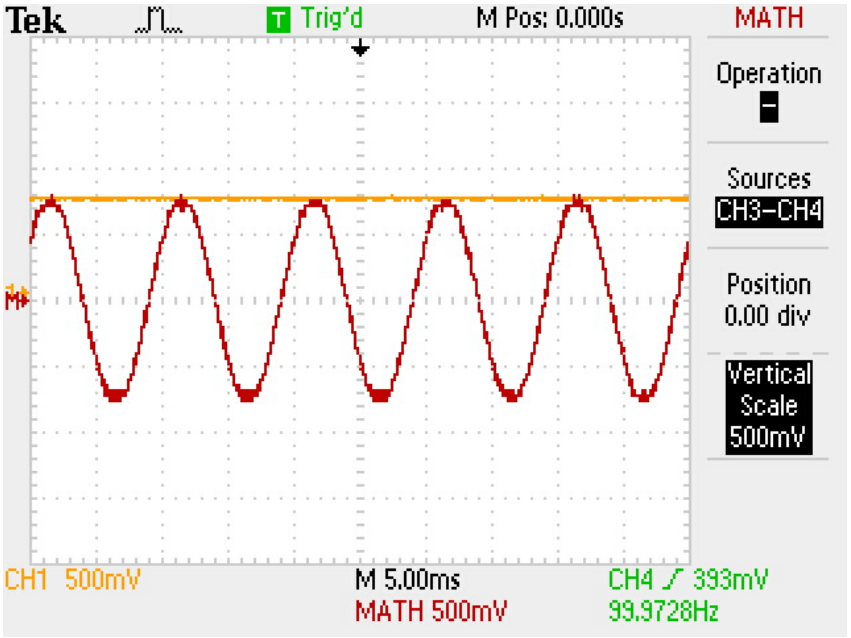

Figure 4.14: Input and output signals when capacitor added to passive MOSFET rectifier

Chapter 5

Conclusion and Future Work

5.1 Conclusion

In Chapter 1, we presented the fundamentals of energy harvesters and energy harvesting. The scales and types of energy harvesting were also discussed in this chapter.

In Chapter 2, power conditioning in vibration-based energy harvesters was introduced, and the Maximum Power Transfer Theorem was discussed. The basic concepts of AC-DC conversion were noted, and different types of rectifiers were reviewed, alongside studying the their rectified signal calculations. There are some commonly-used components in power conditioning circuits; the three components used the most, namely diodes, transformers, and capacitors, were studied in this chapter.

Four different types of rectifiers were simulated in Chapter 3, which are the silicon diode bridge rectifier,the Schottky diode bridge rectifier, and passive and active MOSFET bridge rectifiers. The simulation was done using LTspice IV. Based on simulated data, we calculated voltage and power efficiency for each case at different input voltages. Based on these calculated efficiencies, we made a comparison in Chapter 3.

In Chapter 4, the natural frequency of the electromagnetic harvester was found under three different conditions. For the case where the harvester was itself tested

without any connection, the natural frequency was found to be around 56Hz. This natural frequency did not significantly change when we connected the rectifier to the harvester.

We also tested the rectifier with a harvester to determine the optimum load, which is important to transfer maximum power between media. The optimum load is 24 Ω when the harvester itself is connected directly to the load, whereas it is 46 Ω when the rectifier is connected to the harvester. With rectifier connection the optimum load is doubled.

We also measured the input impedance of the rectifier in Chapter 4. The rectifier was tested with the harvester for different g values, and power efficiency vs acceleration was calculated.

In Chapter 4, we finally discussed the PCB design, and after the PCB was fabricated and assembled, we tested it with and without a capacitor at the end.

5.2 Future Work

In this work we showed that MOSFET-type full-wave rectifiers are more efficient than diode-types, and there is no need for a transformer, which can be very troublesome for harvester systems because of its weight and size. We found over 80% voltage efficiency at a 500 mV input amplitude, without using any transformer and using off-the-shelf components.

As we showed in the simulation, below a 600 mV input, the Schottky diode bridge rectifier has the best voltage and power efficiency, whereas above a 600 mV input amplitude, MOSFET-type rectifiers are more efficient. As a future work, parallel system could be used, and below 600 mV a Schottky diode rectifier can be used, and above 600 mV a passive MOSFET rectifier can be used as a rectifier. By doing this we can have over 30% efficiency in a wider range of input voltages.

Also, since we did not test our system with actual electronic loads, like a sensor node or a transmitter, we could test our system with these loads, and study the working behaviour under these conditions.

References

[1] S. Beeby, and N. White *Energy Harvesting for Autonomous Systems*, Artech House, 2010.

[2] J.R. Fernandes, M. Martins,and M. Piedade, "An Energy Harvesting Circuit for Self-Powered Sensors" *17th International Conference "Mixed Design of Integrated Circuits and Systems"*, Wroclaw, Poland, 2010.

[3] M. D. Seeman, S. R. Sanders,and J. M. Rabaey, "An Ultra-Low-Power Power Management IC for Energy-Scavenged Wireless Sensor Nodes" *Proc. IEEE Power Electron. Spec. Conf.*, pp.925-931, 2008

[4] J.P. Thomas, M.A. Qidwai, and J.C. Kellogg, "Energy Scavenging for small-scale unmanned systems ", *IEEE Journal of Power Sources*, Volume 159, pp. 1494-1509, 2006.

[5] D. Brunelli, C. Moser, L. Thiele, and L. Benini, "Design of a Solar-Harvesting Circuit for Batteryless Embedded Systems" *IEEE Transcactions on Circuits and Systems*, Volume 56, pp. 2519-2528, 2009.

[6] N. Kong, and D. S. Ha, "Low-Power Design of a Self-powered Piezoelectric Energy Harvesting System With Maximum Power Point Tracking" *IEEE Transactions on Power Electronics*, Volume 27, pp. 2298-2308, 2012.

[7] R. J. M. Vullers, R. van Schaijk, I. Doms, C. van Hoof, and R. Mertens, "Micropower Energy Harvesting" *Solid-State Electronics*, Volume 53, pp. 684-693, 2009

[8] E. O Torres, and G. A. Rincon-Mora, "Self-Tuning Electrostatic Energy-Harvester IC" *IEEE Transactions on Circuits and Systems*, Volume 57, pp. 808-812, 2010.

[9] J.M. Gilbert, and F. Balouchi, " Comparison of Energy Harvesting Systems for Wireless Sensor Networks" *International Journal of Automation and Computing*, Volume 5, pp. 334-347, 2008.

[10] G. K. Ottman, H. F. Hofmann, A. C. Bhatt, and G. A. Lesieutre, "Adaptive Piezoelectric Energy Harvesting Circuit for Wireless Remote Power Supply" *IEEE transaction on Power electronics*, Volume 17, pp. 669-676, 2002.

[11] A. Khaligh, P. Zeng, and C. Zheng, "Kinetic Energy Harvesting using piezoelectric and Electromagnetic Technologies-state of the art" *IEEE Transactions on Industrial Electronics* Volume 57, no. 3 pp. 850-860, 2010.

[12] M. Kiziroglu, C. He, and E. Yeatman, "Rolling Rod Electrostatic microgenerator" *IEEE Transactions Industrial Electronics*, Volume 56, no. 4, pp. 1101-1108, 2007.

[13] A. Tabesh, and L. Frechette, "A Low-power Stand-alone Adaptive Circuit for Harvesting Energy from A Piezoelectric Micropower Generator" *IEEE Transactions Industrial Electronics*, Volume 57, no. 3, pp. 840-849, 2010.

[14] J. Colomer, J. Brufau, P. Miribel-Catala, A. Saiz-Vela, M. Puig-Vidal, and J. Samitier, "Power Conditioning Circuitry for A Self-powered System Based On micro PZT Generators in a 0.13μM Low-voltage Low-power Technology", *Proc. IEEE Int. Trans. Ind. Electron.*, pp. 2353-2357, 2007.

[15] S. Mehraeen, S. Jagannathan, and K. Corzine, "Energy Harvesting From Vibration With Alternate Scavenging Circuitry and Tapered Cantilever Beam" *IEEE Transaction on Industrial Electronics*, Volume 57, pp. 820-830, 2010.

[16] A. Kempitiya, D.-A. Borca-Tasciuc, and M. M. Hella, "Analysis and Optimization of Asynchronously Controlled Electrostatic Energy Harvesters" *IEEE Trans. on Industrial Electronics*, Volume 59, no. 1, pp. 456-463, 2012.

[17] B. H. Stark, P. D. Mitcheson, P. Miano, T. C. Green, E. M. Yeatman, and A. S. Holmes, "Converter Circuit Design, Semiconductor Device Selection and Analysis of Parasitic for Micropower Electrostatic Generators" *IEEE Transaction on Power Electronics*, Volume 21, no. 1, pp.27-37, 2006.

[18] M.R. Patel, *Wind and Solar Power Systems*, CRC Press LLC, Boca Raton, FL, 1999.

[19] C. Lu, V. Raghunathan, and K. Roy,"Efficient Design of Micro-Scale Energy Harvesting Systems", *IEEE Journal on Emerging and Selected Topics in Circuits and Systems*, Volume 1, no. 3, pp. 254-266, 2011.

[20] L. Mateu, and F. Moll, "Review of Energy Harvesting Techniques and Applications for Microelectronics" *In Proceedings of SPIE- The International Society for Optical Engineering, VLSI Circuits and Systems II*, Volume 5837, pp. 359-373, 2005.

[21] M. Yilmaz, E. M. Abdel-Rahman, S. Park, K. Elrayes, M. Yavuz, M. A. E. Mahmoud, M. S. M. Soliman, and R. A. Elshatshat, "Testing of a passive full-wave MOSFET rectifier" *Proceeding of the 24th CANCAM* Saskatoon, Saskatchewan, Canada, June 2013

[22] N. S. Shenck, and J. A. Paradiso, " Energy Scavenging with Shoe-Mounted Piezoelectrics," *IEEE Micro* Volume 21, pp. 30-42, 2001

[23] K. El-Rayes, "Low-Frequency Electromagnetic Energy Harvesting ", *MS. thesis, University of Waterloo*, 2011.

[24] N. Kong, D.S. Ha, A. Erturk, and D.J. Inman, " Resistive impedance matching circuit for piezoelectric energy harvesting" *J. Intell. Mater. Syst. Struct.* Volume 21, pp. 1293-1302,2010.

[25] http://www.electricityforum.com/products/trans-s.htm .

[26] T.T. Le, J. Han, A.V. Jouanne, K. Mayaram, T.S, and Fiez, "Piezoelectric Micro-power generation interface circuits," *IEEE J. Solid-State Circuits*, Volume 6, pp. 1411-1420, 2006.

[27] C. Peters, O. Kessling, F. Henrici, M. Ortmanns, and Y. Manoli, "CMOS integrated highly efficient full wave rectifier," *Proc. IEEE Int. Symp. Circuits syst.*, pp. 2415-2418, 2007.

[28] S. Hashemi, M. Sawan, and Y. Savaria, "A novel low drop CMOS active rectifier for RF-powered devices:Experimental results," *Microelectron.J,* Volume 40, pp. 1547-1554, 2009.

[29] Y. K. Ramadass, and P. C. Chansdrakasan, "A Battery-Less Thermoelectric Energy Harvesting Interface Circuit With 35 mV Startup Voltage," *IEEE Journal of Solid-State Circuits,* Volume 46, no 1, pp. 333-341, 2011.

[30] H. Kim, S. Priya, H. Stephanou, and K. Uchino, "Consideration of impedance matching techniques for efficient piezoelectric energy harvesting," *IEEE Trans. on ultrasonics, ferroelectrics, and frequency control*, Volume 54, pp. 1851-1859, 2007.

[31] P.P. Proynov, G.D. Szarka, B.D. Stark, and N. McNeil, "Resistive matching with a feed-forward controlled non-synchronous boost rectifier for electromagnetic energy harvesting" *IEEE APEC 2013* Long Beach, USA, March 2013,

[32] http://www.docstoc.com/docs/127650863/Half-Wave-Rectifier-Theory .

[33] M. H Rashid, *Power Electronics Handbook*, Academic Press, 2001.

[34] http://en.wikipedia.org/wiki/Transformer .

[35] http://forum.allaboutcircuits.com/showthread.php?t=56064 .

[36] "NTJS3157N-Trench Power MOSFET datasheet" *ON Semiconductor* Rev. 2, February, 2006.